Current analytical methods and applications used in the insight of serum proteins interactions with various food additives, pesticides, and contaminants

Cem Erkmen[1*] , Md. Zahirul Kabir[2*]

[1]Department of Analytical Chemistry, Faculty of Pharmacy, Istanbul Aydin University, Istanbul 34295, Türkiye
[2]Department of Analytical Chemistry, Faculty of Pharmacy, Ankara University, Ankara 06560, Türkiye

*Correspondences: Cem Erkmen, Department of Analytical Chemistry, Faculty of Pharmacy, Istanbul Aydin University, Besyol Mah. Inönü Cd. No 38, Istanbul 34295, Türkiye. cmrkmn@gmail.com; Md. Zahirul Kabir, Department of Analytical Chemistry, Faculty of Pharmacy, Ankara University, Emniyet Mah. Dögol Cd. No 4, Ankara 06560, Türkiye. mmbzahirulkabir@gmail.com
Academic Editor: Zhaowei Zhang, Chinese Academy of Agricultural Sciences, China
Received: December 25, 2023 **Accepted:** February 24, 2024 **Published:** May 24, 2024

Abstract

In recent years, many societies have expressed increasing apprehension regarding the potential negative impacts of food additives, pesticides, and environmental contaminants on human health. Environmental or occupational exposure to these compounds can cause significant adverse effects on human health by causing temporary or permanent changes in the immune system. There is supporting evidence linking pesticides/food ingredients/contaminants-induced immune alterations to the prevalence of diseases associated with changes in immune responses. Hence, it is essential to comprehensively understand the key mechanisms contributing to immune dysregulation induced by these substances, including direct immunotoxicity, endocrine disruption, and antigenicity. The impact of pesticides/food ingredients and contaminants on the human body ranges from mild to severe, depending on their affinity for blood components. These compounds form complexes with blood serum proteins, influencing their metabolism, transport, absorption, and overall toxicity. Numerous studies in the literature have explored the interactions between serum proteins and various molecules, including pesticides, drugs, and food dyes. These investigations employed a range of techniques, including spectroscopy, electrochemical and chromatographic methods as well as molecular modeling and molecular dynamics simulations analyses. This recent review, spanning from 2020 to the present, has been employed to investigate the binding characteristics, mechanisms, and attributes of different food additives, pesticides, and contaminants with serum proteins by using various techniques such as steady-state fluorescence, circular dichroism and ultra-violet spectroscopies, and computational docking methods. The review provides insights into these compounds' positions and affinities to proteins and possible effects on human health through detailed research studies.

Introduction

Nowadays, a substantial growth in population and the swift advancement of global industrialization are associated with a rise in the release of various hazardous and harmful substances. Hazardous pollutants like dyes, heavy metals, fertilizers, pesticides, personal care products, food additives, nitrophenols, and medications are upsetting the balance of nature and generating environmental toxins at a disturbing pace. Therefore, due to significant ecological risks and adverse effects on human health, the pervasive existence and capacity of hazardous pollutants to infiltrate the environment have garnered widespread public attention in recent years. A comprehensive categorization and impact of these hazardous pollutants is shown below (Figure 1) [1].
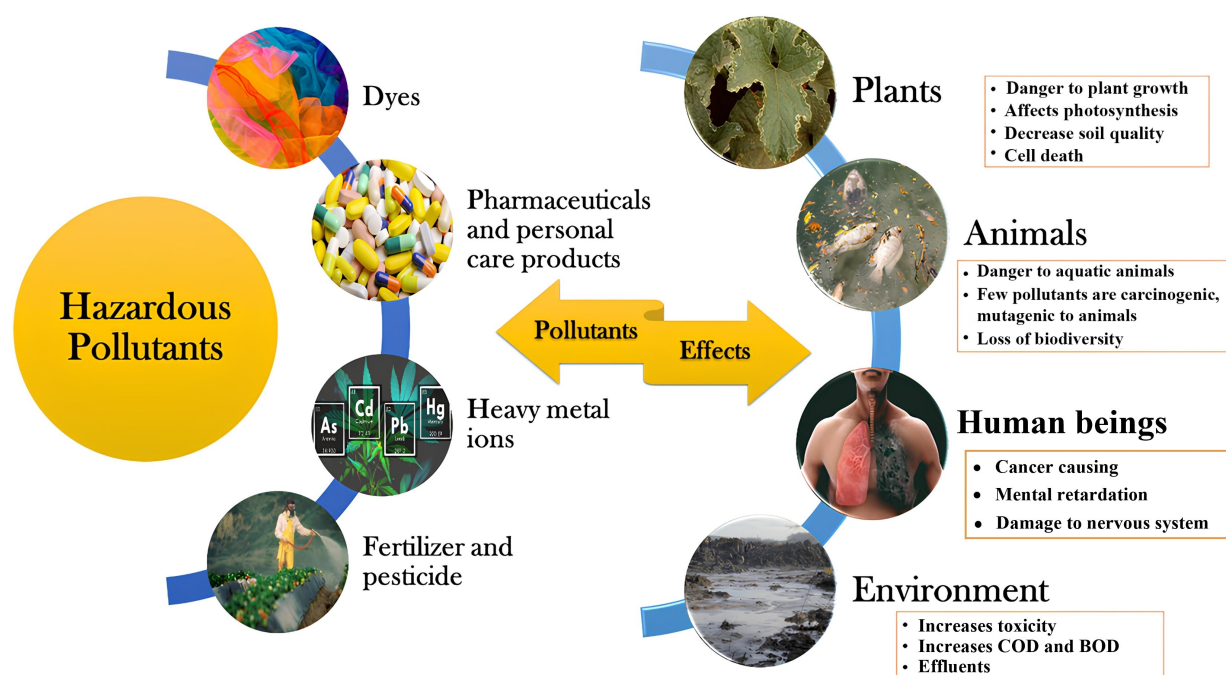

Figure 1. Broad classification and effects of hazardous pollutants. COD: chemical oxygen demand; BOD: biochemical oxygen demand

Note. Adapted from "Critical review on hazardous pollutants in water environment: occurrence, monitoring, fate, removal technologies and risk assessment," by Rathi BS, Kumar PS, Vo DN. Sci Total Environ. 2021;797:149134 (https://doi.org/10.1016/j.scitotenv.2021.149134). © 2021 Elsevier B.V.

Because certain non-biodegradable organic pollutants persist in the environment for extended periods, the accumulation of these contaminants in living organisms ultimately infiltrates the food chain, significantly impacting the ecosystem. Specifically, organic contaminants like nitrophenols find extensive use in the production of pharmaceuticals, dyes, a variety of pesticides, and explosives. Due to their high acidity, water solubility, non-biodegradability, and carcinogenic properties, the unregulated utilization and release of these substances into the environment, without proper treatment, are leading to significant health concerns [2–5]. Furthermore, several neurotoxic and deadly pesticides are being widely employed to reduce crop losses by eradicating weeds and eliminating pests. In addition to impacting the reproductive and immune systems, the persistent consumption of food and water contaminated with pesticides is giving rise to various metabolic diseases [1–6]. While the primary purpose behind the utilization of food additives, whether natural or chemically synthesized, was to prolong shelf life and enhance the color, fragrance, taste, and nutritional value of food, their excessive use has posed a threat to human life. Natural food additives are predominantly produced by refining components extracted from plants or animals, while chemical food

additives necessitate the use of chemical raw materials for their production. The food industry relies significantly on the application of chemical additives, but their overuse is a factor contributing to a range of gastrointestinal, neurological, and immunological diseases. The impacts of various contaminants and food additives on mental disorders are explored in the following sections and summarized in Figure 2 [7–10].
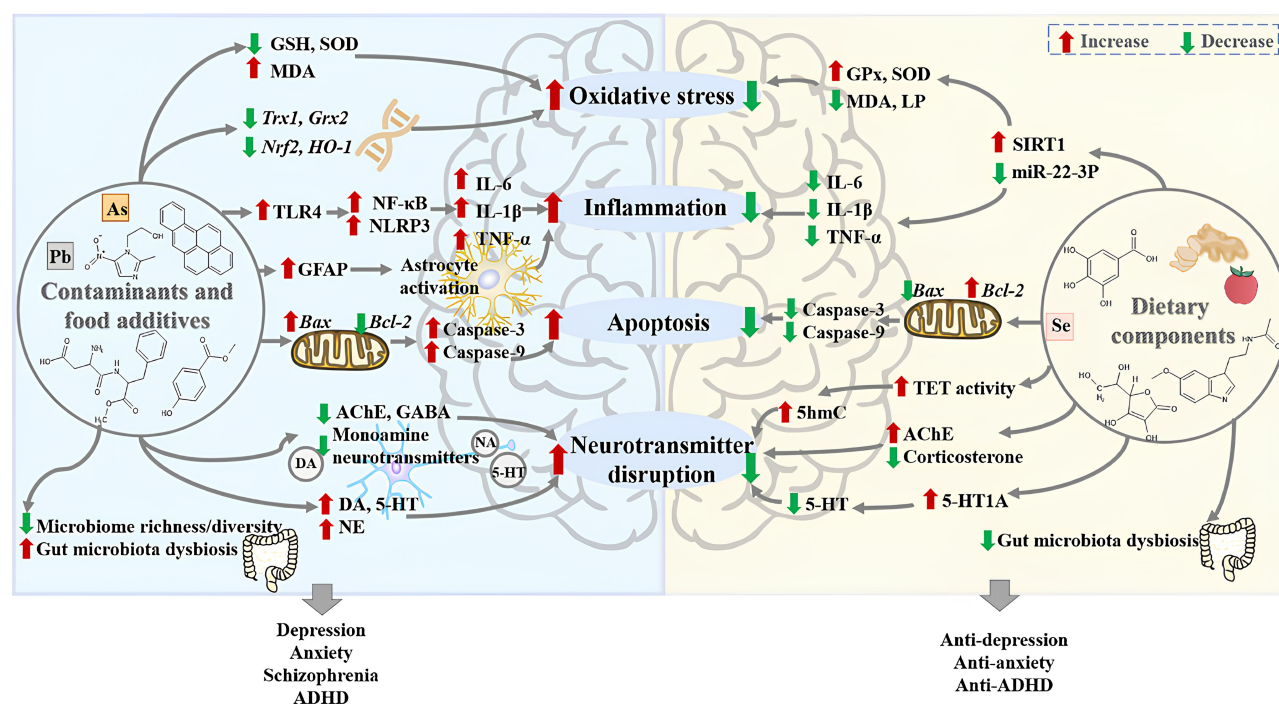

Figure 2. The harmful effects of contaminants and food additives on mental disorders as well as the protective effects of foods and dietary components against them, which is retrieved from the literature. The potential mechanisms of the harmful effects of contaminants and food additives on mental disorders include: (1) the contaminants and food additives could increase oxidative stress in the brain through increasing the level of malondialdehyde (MDA), decreasing levels of glutathione (GSH) and superoxide dismutase (SOD), and inhibiting the expression of antioxidant genes thioredoxin 1 (*Trx1*) and glutaredoxin 2 (*Grx2*), as well as the messenger RNA (mRNA) expression of nuclear factor erythroid 2 related factor 2 (Nrf2) and heme oxygenase-1 (HO-1); (2) the contaminants and food additives could induce neuroinflammation by activating astrocytes, enhancing the protein expression of Toll-like receptor 4 (TLR4), nuclear factor-kappa B (NF-κB), and nucleotide-binding domain and leucine-rich repeat related (NLR) family, pyrin domain containing 3 (NLRP3), and increasing the levels of pro-inflammatory cytokines interleukin 6 (IL-6), IL-1β, and tumor necrosis factor-alpha (TNF-α); (3) the contaminants and food additives could induce neuronal apoptosis by down-regulating the expression of B cell lymphoma-2 (Bcl-2), up-regulating the expression of Bcl-2-associated X protein (Bax), as well as the protein levels of caspase-3 and caspase-9; (4) the contaminants and food additives could disrupt neurotransmitters, especially monoamine neurotransmitters; (5) the contaminants and food additives could decrease the gut microbiome richness and diversity, as well as cause gut microbiota dysbiosis. Moreover, the potential mechanisms of the protective effects of dietary components against mental disorders caused by contaminants and food additives include: (1) dietary components could decrease oxidative stress in the brain by decreasing the levels of MDA and lipid peroxidation (LP), increasing the activities of SOD and glutathioneperoxidase (GPx) via the microRNA-22-3p (miR-22-3p)/sirtuin 1 (SIRT1) signaling pathway; (2) dietary components could reduce neuroinflammation through decreasing the levels of pro-inflammatory cytokines IL-1β, IL-6, and TNF-α; (3) dietary components could reduce neuronal apoptosis by down-regulating pro-apoptotic proteins caspase-3, caspase-9, and Bax, as well as up-regulating the expression of Bcl-2; (4) dietary components could regulate neurotransmitters by increasing activities of ten-eleven translocation (TET) and 5-hydroxymethylcytosine (5hmC) in the fetal brain, decreasing levels of corticosterone and 5-hydroxytryptamine (5-HT, serotonin); (5) dietary components could reverse gut microbiota dysbiosis caused by contaminants and food additives. AchE: acetylcholinesterase; ADHD: attention deficit hyperactivity disorder; GABA: γ-aminobutyric acid; GFAP: glial fibrillary acidic protein; NA: noradrenaline; NE: norepinephrine; DA: dopamine

Note. Reprinted from "New insights into the protection of dietary components on anxiety, depression, and other mental disorders caused by contaminants and food additives," by Xiong RG, Li J, Cheng J, Wu SX, Huang SY, Zhou DD, et al. Trends Food Sci Technol. 2023;138:44–56 (https://doi.org/10.1016/j.tifs.2023.06.004). © 2023 Elsevier Ltd.

To safeguard consumers from contaminated foods, numerous national and international organizations, such as the European Food Safety Authority (EFSA), World Health Organization (WHO), US Environmental Protection Agency (EPA), and US Food and Drug Administration (FDA), have instituted regulations and guidelines to mitigate exposure to these chemicals. Owing to the efficacy of these regulations and legal frameworks, emissions of dioxins, dioxin-like compounds, and certain hazardous pesticides have notably decreased in recent years. The United Nations Environment Programme (UNEP) global monitoring plan for

persistent organic pollutants has resulted in a consistent reduction in the levels of polychlorinated dibenzo-*p*-dioxins, polychlorinated dibenzofurans, polychlorinated biphenyls, and organochlorine pesticides in human milk. Nevertheless, the implementation of international codes and standards remains challenging, particularly in the face of the ongoing rise in the global population, projected to reach nine billion by 2050 [11–14].

Generally, investigating the binding properties, mechanisms, and characteristics of different food additives, pesticides, and contaminants with serum proteins is important for several reasons summarized below. Understanding the interaction of these substances with serum proteins helps determine their bioavailability. The binding capacity influences how these compounds are transported in the bloodstream and delivered to their target tissues. Additionally, it provides insights into potential toxicity and its impact on overall health [15, 16]. Besides, this information is vital for assessing the potential risks associated with exposure to these compounds. In cases where individuals are simultaneously exposed to pharmaceuticals and contaminants, understanding the binding interactions with serum proteins becomes essential. Because, drug interactions can alter the pharmacokinetics of therapeutic agents, affecting their efficacy and safety. Studying the interactions of contaminants with serum proteins is relevant not only for human health but also for understanding the environmental impact. The fate and transport of contaminants in ecosystems can be influenced by their interactions with proteins, affecting wildlife and ecosystems. In the context of food additives, studying their interactions with serum proteins is crucial for assessing food safety. These researches help to evaluate the potential health risks associated with the consumption of certain food products [17–22].

Therefore, exploring the interactions between these chemicals and human serum proteins is crucial for understanding the distribution, metabolism, and toxicity mechanisms of pollutants at the molecular level. While current research on pollutant toxicity predominantly emphasizes the dose-response relationship and cytotoxic effects on organisms, it is imperative to recognize that the essence of pollutant toxicity lies in the interaction between pollutants and biomolecules. Monitoring these interactions reveals variations in the chemical diversity of pollutant molecular structures, binding modes, binding free energy between pollutants and biomolecules, and significant distinctions in biomolecule conformation [23]. As a pioneering study, this review aims to assemble and combine the existing knowledge from diverse scientific studies, shedding light on the methodologies utilized to elucidate the binding properties, mechanisms, and characteristics of these compounds with serum proteins. By critically examining the analytical techniques, such as spectroscopy, molecular docking, and chromatographic methods, the review seeks to provide a nuanced understanding of molecular interactions. Moreover, the overarching goal is to contribute to the advancement of analytical approaches in this field, fostering a deeper comprehension of the implications of these interactions for human health and the environment. By consolidating the current state of research, the review aims to identify gaps in knowledge, potential areas for future investigation, and applications of these findings in areas such as risk assessment, pharmacokinetics, and the development of therapeutic interventions. In light of these considerations, this review delves into the interaction mechanisms of various food additives, pesticides, and contaminants with different serum proteins. The examination encompasses studies conducted from 2020 to 2023, providing a summary of the analytical and computational techniques employed in these investigations.

Methods employed to study the binding of food additives, pesticides, and contaminants with serum proteins

Basic information about serum proteins

Serum albumin is the predominant protein in blood plasma and is frequently employed as a representative protein in studies investigating molecule/ligand interactions. Human serum albumin (HSA) serves as the primary transport protein in blood plasma, playing a vital role in transporting both endogenous and exogenous ligands, including drugs and metabolites. The extent to which a molecule binds to HSA influences its *in vivo* delivery, distribution, effectiveness, and potential for toxicity [24, 25].

Bovine serum albumin (BSA) stands out as a versatile and widely used protein for different scientific purposes. BSA obtained from bovine blood can be used as a substitute for HSA in many experimental studies due to its structural similarity to HSA and its low cost. BSA was found wide application in protein quantitative analysis, in preserving the solubility and activity of enzymes and other biomolecules, and in immunoassays due to its inert nature as an ideal blocking agent. Additionally, BSA is a common component in cell culture media and provides essential nutrients and proteins to support cell growth due to its consistent and well-characterized composition [26, 27].

Human hemoglobin (Hb) stands out as a vividly red tetrameric protein, equipped with four oxygen-binding sites. Its primary role involves the transportation of oxygen, electrons, H^+, CO_2, and 2,3-bisphosphoglycerate within the bloodstream. While the structural and functional aspects of Hb have undergone comprehensive scrutiny, investigations into its interactions with various molecules have been largely confined to a subset of small compounds. Examining the interplay between Hb, a key physiologically active protein, and clinically relevant small molecules presents an opportunity to glean insights into Hb-mediated drug targeting. The exploration of bimolecular interactions involving proteins akin to Hb and specific small compounds holds significant promise within the field of biology, offering the potential to uncover novel perspectives on therapeutic strategies and drug design [28, 29].

Another serum protein, lysozyme, although not a dominant protein in the blood system, exhibits unique properties and plays an important role in maintaining homeostasis. The presence of lysozyme in blood, which is typically found in higher concentrations in body fluids such as tears and saliva, indicates the potential importance of this protein in immune defense. Owing to its antimicrobial properties, this protein may contribute to the innate immune response by disrupting bacterial cell walls. Although its concentration in the blood is lower compared to other blood proteins, the enzymatic activity of lysozyme makes it an effective protein in fighting infections and supporting general immune function in the bloodstream [30, 31].

Studying the interactions of all the above-mentioned proteins with different molecules provides information in terms of understanding potential or undesirable side effects, general kinetics of the compounds in the body, optimizing new molecular formulations, and distribution strategies in the body. For this reason, many different analytical techniques are frequently used to elucidate the interactions of serum proteins with molecules.

Basic information about analytical methods

Ultraviolet (UV)-visible (UV-Vis) absorption spectroscopy stands as a crucial and basic technique for discerning the interaction and complex formation of small molecules with serum proteins. Examining alterations in the absorbance profile of protein using UV-Vis absorption spectroscopy provides a comprehensive understanding of molecular interactions. Moreover, utilizing the Benesi-Hildebrand equation, the binding constant or association constant is calculated from UV-Vis absorption data, providing quantitative insights into molecule/ligand interactions with serum proteins [32, 33].

Fluorescence spectroscopy emerges as a highly sensitive and selective method for investigating the interactions between proteins and molecules. The intrinsic fluorescence spectra of proteins, mainly derived from aromatic amino acids such as tryptophan (Trp) and tyrosine residues, serve as a valuable indicator of structural changes induced by varying molecule concentrations. Quenching or enhancement mechanisms, generally categorized as static, dynamic, or mixed, can be easily interpreted from fluorescence data. Stern-Volmer and double logarithmic plots along with relevent equations provide quantitative data such as the Stern-Volmer constant, bimolecular quenching rate constant, binding constant, and the number of binding sites for the quenching or enhancement process. Thermodynamic parameters, such as entropy change, and enthalpy change offer insights into the non-covalent forces governing serum protein interactions. Calculated values and signs using the van't Hoff equation, these parameters help identify the predominant stabilizing forces, whether electrostatic interactions, hydrophobic interactions, or hydrogen bonding and van der Waals interactions. Therefore, fluorescence spectroscopy emerges as a powerful tool not only for understanding molecular interactions but also for unraveling the thermodynamics behind these intricate binding processes. Furthermore, electron emission matrix spectroscopy, commonly referred to as three-

dimensional fluorescence spectroscopy, has gained prominence as a scientific tool for scrutinizing the interaction mechanisms between molecules and serum proteins. This technique has emerged as a valuable resource in recent years, facilitating a comprehensive analysis of the microenvironment and conformational alterations within the structure of serum proteins induced by the presence of molecules. Its application provides a three-dimensional perspective, enhancing insights into complex molecular dynamics (MD) simulations involved in the interaction between serum proteins and molecules [34, 35].

The formation of complexes between serum proteins and molecules gives rise to energy transfer phenomena, involving the exchange of energy between serum proteins and interacting molecules. This energy transfer efficiency is elucidated through Förster (fluorescence) resonance energy transfer (FRET), a mechanism that entails the non-radiative transfer of energy from a donor fluorophore to an acceptor molecule. The success of FRET relies on specific conditions: proximity between the excited fluorophore (donor) and the drug/ligand (acceptor), overlap of the donor's fluorescence emission spectrum with the acceptor's excitation wavelength, correct orientation of the dipole moments of donor and acceptor molecules, and a high quantum yield of the donor [36, 37].

As another analytical tool, circular dichroism (CD) spectroscopy stands as a widely utilized method for examining alterations in the secondary and tertiary structures of serum protein induced by the presence of molecules. Specifically, changes in the secondary structure can be observed in the far-UV region of the CD spectra, where the serum protein CD spectra typically exhibit bands at different regions, indicative of α-helical content. These bands serve as highly sensitive markers for the binding of molecules. Increases or decreases in the intensity of the peaks of these bands provide information about the dynamic structural changes caused by the interaction. Moreover, the CD data can be further represented as mean residue ellipticity (MRE), offering a quantitative measure of the CD signal [32, 38].

Isothermal titration calorimetry (ITC) represents a widely employed technique for investigating the interactions between a protein and a molecule, providing insights into the energetics of complex formation. Through the measurement of energy changes during the process, ITC enables the determination of various thermodynamic parameters crucial for understanding the interaction between the molecules and serum proteins. Calculations involving changes in enthalpy, entropy, and the number of binding sites offer valuable information about the nature of the forces driving the complex formation [32, 39].

Fourier transform infrared (FTIR) spectroscopy serves as a crucial technique for revealing information about the functional groups within a molecule, producing a spectrum that acts as a unique molecular fingerprint. Specifically, FTIR proves valuable in characterizing secondary structural changes in proteins, both before and after binding with a molecule. FTIR not only facilitates qualitative observation but also enables quantitative analysis of changes in the secondary structure, including the amide I (C=O stretching) and amide II (C-N stretching coupled with N-H bending mode) bands, following the binding of a molecule [40, 41].

Nowadays, molecular docking stands as a crucial tool for unraveling the intricate interactions between small molecules and macromolecules, such as proteins and DNA, playing a pivotal role in rational drug/ligand design and development based on molecular structures. These studies offer predictive insight into the binding modes of drugs/ligands with macromolecules, allowing for informed decisions before embarking on experimental studies. Molecular docking not only validates findings obtained in the laboratory but also contributes to a deeper understanding of the binding orientation. Automated software facilitates these studies, predicting binding modes, and energetically favorable conformations between molecules and serum proteins. The process of molecular docking commences with acquiring the three-dimensional Protein Data Bank (PDB) structure of the macromolecule from databases like research collaboratory for structural bioinformatics or others, while molecule structures can be obtained from repositories like PubChem or ChemSpider. Multiple software options are available for docking studies, including AutoDock 4.0, AutoDock 4.2, AutoDock Vina, Hex 8.0, BSP SLIM online, and more. AutoDock, in particular, is widely employed for its reliability in predicting energetically favorable conformations. The selection of the energetically favorable conformer, typically the run with the lowest binding energy, allows

for flexibility in drug/ligand docking, incorporating detailed molecular mechanics to calculate energy within the assumed active site [32, 42, 43].

MD simulations have proven to be a powerful tool for comprehending the intricate relationships between macromolecular structure and function. This computational approach calculates the time-dependent behavior of molecular systems, offering crucial insights for molecule design. MD simulation studies provide a detailed understanding of variations, stability, thermodynamics, and conformational changes within the structure of macromolecules in the presence of molecules. The binding of a molecule to a protein induces measurable conformational changes, quantified through root mean square deviation (RMSD), root mean square fluctuation (RMSF), radius of gyration (R_g), and formed hydrogen bonds [32, 42, 44].

Potential findings and latest applications of serum protein binding

Currently, numerous studies focus on residue detection and degradation methods of pesticides, environmental pollutants, and food products or their degradation metabolites. However, there is a notable scarcity of research on the toxicity mechanisms and transport properties of these compounds and metabolites in organisms. Therefore, in recent years, efforts have been made to investigate the binding interaction mechanisms of these substances with human serum proteins, especially in humans. In 2023, in their research, Cui et al. [45] explored the binding interaction mechanisms between HSA and the main degradation metabolites of pyrethroid insecticides, namely, 3-phenoxybenzoic acid (3-PBA) and 4-fluoro-3-PBA (4-F-3-PBA), through a combination of theoretical simulations and experimental validation. In this study, for fluorescence spectrum experiments, encompassing both fluorescence quenching and competitive binding experiments, HSA solutions were blended with two distinct small molecule solutions, maintaining an HSA concentration of 2 μmol/L and varying the small molecule concentrations from 0 μmol/L to 6 μmol/L. Following a 30 min water bath at temperatures of 298 K, 303 K, and 310 K, the fluorescence emission spectrum within the 290–450 nm range was scanned at a speed of 2,000 nm/min with an excitation wavelength of 280 nm. Steady-state fluorescence spectra revealed a static fluorescence quenching mechanism. Based on the binding constants, it was observed that 4-F-3-PBA (1.53×10^5 L/mol) exhibited a stronger binding affinity to HSA than 3-PBA (1.42×10^5 L/mol) at subdomain IIA (site I) (Figure 3). UV absorption and CD spectra indicated that the metabolites induced subtle changes in the microenvironment and conformation of HSA. Moreover, ITC revealed that the metabolites and HSA exhibited spontaneous combination primarily through hydrogen bonding and van der Waals interactions. Also, molecular docking analyses validated the aforementioned findings. To sum up, the toxicity characteristics of the metabolites were subjected to additional analysis using software, revealing that 4-F-3-PBA exhibited higher toxicity compared to 3-PBA. Given the widespread exposure of these metabolites in food, the environment, and the human body, there is a compelling need for further investigation into the toxicity of pyrethroid insecticide metabolites [45].

In another study conducted in 2023, Yang et al. [46] aimed to investigate the pH-dependent binding mechanisms between cyandin-3-*O*-glucoside (C3G) and BSA, exploring the interactions of natural pigments, anthocyanins, with proteins under varying pH conditions. Fluorescence quenching experiments and microscale thermophoresis (MST) analyses revealed a pH-dependent binding affinity, with the order pH 7 > pH 5 > pH 3, and dissociation constants (K_d) of 43.1 μmol/L (fluorescence quenching) and 33.0 μmol/L (MST) at pH 7. The prevailing forms of C3G were determined through UV-Vis absorption spectra with pH-jump experiments. Moreover, CD, Trp fluorescence, zeta potential, and particle size measurements indicated the "molten globule" state of BSA at pH 3, with C3G having a negligible effect on BSA conformation. MD simulations were employed to investigate the binding mechanisms, emphasizing the significance of electrostatic interaction. The flavylium cation exhibited limited binding to BSA at pH 3 due to electrostatic repulsion. In contrast, uncharged forms of C3G at all pH values bound to the BSA surface through hydrophobic interactions and hydrogen bonds, possibly in a weak and nonspecific manner. Anionic quinoidal bases, prevalent C3G forms at pH 7, predominantly bound to positively charged pockets on BSA, establishing several hydrogen bonds with surrounding amino acids, resulting in enhanced binding affinity [46].
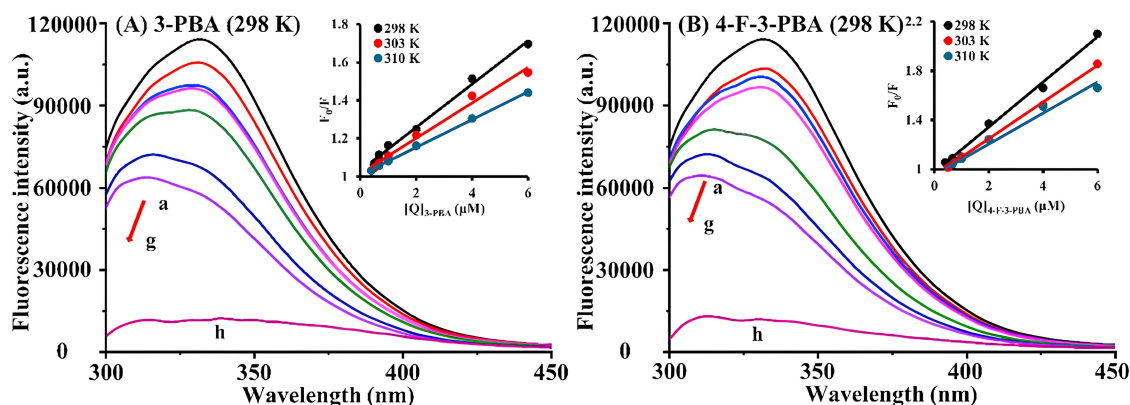
Figure 3. Fluorescence emission spectra of HSA with varying concentrations of 3-PBA and 4-F-3-PBA. (A) 3-PBA, temperature = 298 K, HSA = 2 μml/L (a–g), 3-PBA = 0–6 μmol/L (a–g), 3-PBA = 2 μmol/L (h); (B) 4-F-3-PBA, temperature = 298 K, HSA = 2 μml/L (a–g), 4-F-3-PBA = 0–6 μmol/L (a–g), 4-F-3-PBA = 2 μmol/L (h). a.u.: arbitrary units

Note. Reprinted from "Exploring the binding mechanism and adverse toxic effects of degradation metabolites of pyrethroid insecticides to human serum albumin: multi-spectroscopy, calorimetric and molecular docking approaches," by Cui Y, Sun Y, Yu H, Guo Y, Yao W, Xie Y, et al. Food Chem Toxicol. 2023;179:113951 (https://doi.org/10.1016/j.fct.2023.113951). © 2023 Elsevier Ltd.

Luteolin and naringenin are flavonoids found extensively in various foods and beverages, and they are also constituents of specific dietary supplements. With a significant consumption of these flavonoids, their sulfate and glucuronide conjugates can accumulate to micromolar concentrations in the bloodstream. Some investigations have delved into specific pharmacokinetic interactions associated with luteolin and naringenin; however, detailed information on their metabolites is limited in existing studies. In a study conducted by Kaci et al. [47], the interactions involving sulfate and glucuronic acid conjugates of luteolin and naringenin were explored concerning their binding to HSA, cytochrome P450 enzymes (CYP2C9, 2C19, and 3A4), and organic anion-transporting polypeptide transporters (OATP1B1 and OATP2B1). In fluorescence experiments (Figure 4), each examined flavonoid exhibited a concentration-dependent reduction in the emission signal of HSA at 340 nm. Both Stern-Volmer plots and Hyperquad assessments indicated a 1:1 stoichiometry of complex formation. Luteolin exhibited a higher affinity for protein binding compared to naringenin. Among the tested flavonoids, luteolin-7-glucuronide (L7G) displayed a significantly decreased binding affinity, which further diminished in the presence of a second glucuronic acid substitution at position 3' (LdG). However, luteolin-3'-glucuronide (L3'G) exhibited a binding constant similar to that of the parent flavonoid. The presence of a sulfate substituent at position 3' (LS) increased the binding affinity toward HSA. For naringenin, glucuronide conjugation markedly reduced the stability of albumin complexes, while sulfate substitution led to a slight enhancement in the binding affinity. Finally, researchers revealed that conjugated metabolites of luteolin and naringenin may exert a significant influence on the pharmacokinetic interactions of these flavonoids [47].

Despite the recognized health benefits of phenolic acids, their interactions with proteins remain unclear. In 2023, Zhang et al. [48] investigated the interactions between BSA and chlorogenic acid (CHA), caffeic acid (CA), as well as their Al^{3+} and Cu^{2+} complexes, utilizing UV-Vis, fluorescence, and CD spectroscopy. Significantly, the binding affinities for BSA were increased with the esterification of the carboxyl group of CA with quinic acid. Furthermore, upon chelation with Cu^{2+} and Al^{3+}, both CHA and CA demonstrated enhanced binding affinities for BSA. Additionally, CHA demonstrated the ability to form CHA-Cu_2 and CHA-Al_2 complexes with Cu^{2+} and Al^{3+}. The results from CD spectroscopy suggested that the interaction between CHA and Al^{3+} with BSA contributed to the folding of BSA's secondary structure. Furthermore, the presence of CHA induced conformational changes in BSA when binding with Al^{3+} [48].

In 2022, Hoseyni et al. [49] explored the interaction between ten synthetic food dyes (Quinoline Yellow, Sunset Yellow, Carmoisine, Amaranth, Red 2G, Allura Red AC, Patent Blue V, Brilliant Blue FCF, Food Green S and Fast Green) and HSA through fluorescence spectroscopy, bio-partitioning micellar chromatography (BMC), and molecular docking analyses. The findings from fluorescence spectroscopy revealed a pronounced quenching effect on the intrinsic fluorescence of HSA, indicating a strong interaction near the Trp-214 residue of HSA. The modified Stern-Volmer equation was employed to calculate the K_b
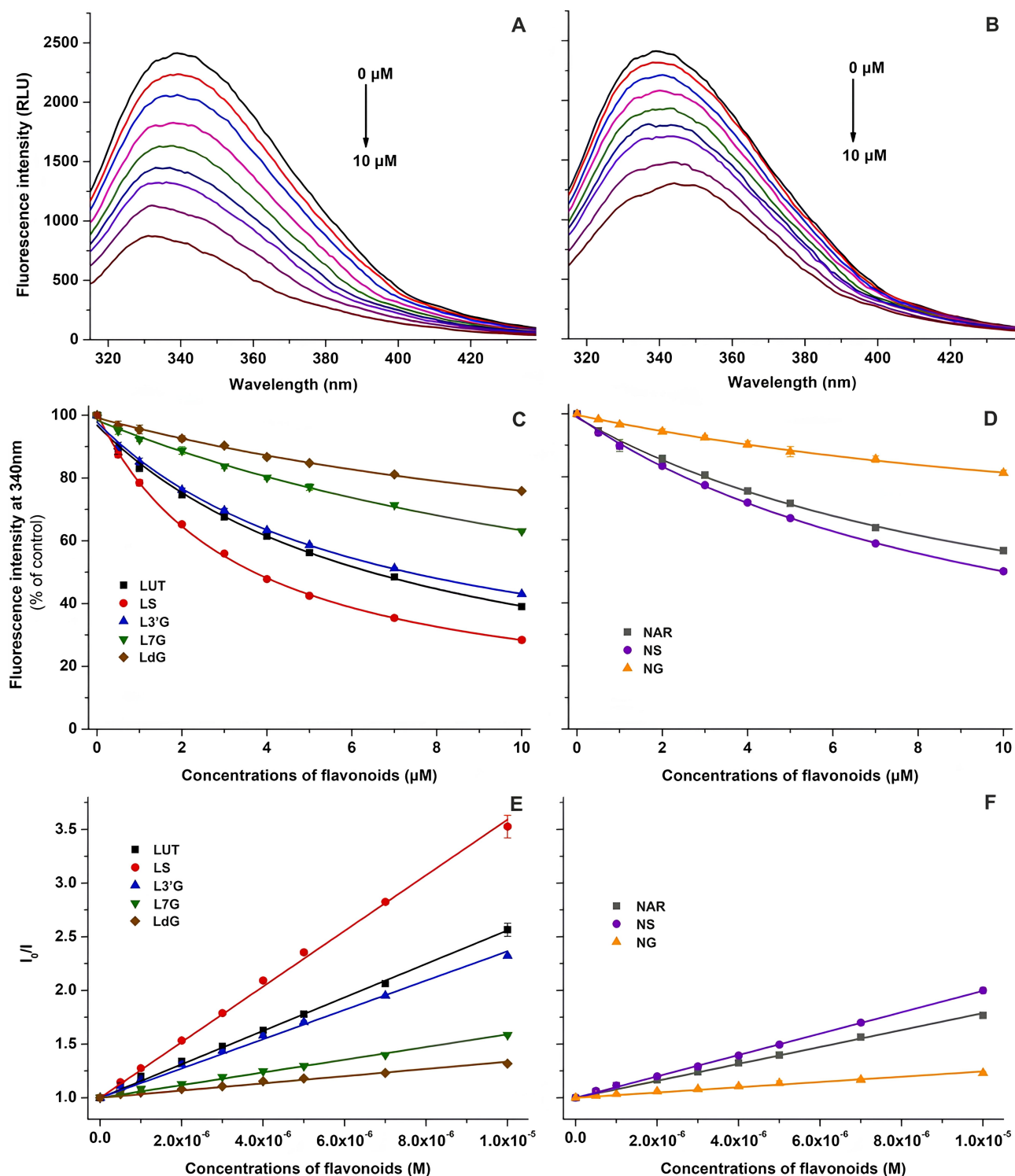
Figure 4. Fluorescence experimental results. (A) Representative fluorescence emission spectra of HSA (2 μmol/L) in the presence of increasing concentrations (0–10 μmol/L) of luteolin (LUT) in phosphate buffer saline [PBS, pH 7.4; excitation wavelength (λ_{ex}) = 295 nm]; (B) representative fluorescence emission spectra of HSA (2 μmol/L) in the presence of increasing concentrations (0–10 μmol/L) of naringenin (NAR) in PBS (pH 7.4; λ_{ex} = 295 nm); (C) flavonoid-induced decrease in the fluorescence emission signal of HSA at 340 nm for LUT, LS, L3'G, L7G, and LdG; (D) flavonoid-induced decrease in the fluorescence emission signal of HSA at 340 nm for NAR, NS, and NG; (E) Stern-Volmer plots of flavonoid-HSA complexes for LUT, LS, L3'G, L7G, and LdG; (F) Stern-Volmer plots of flavonoid-HSA complexes for NAR, NS, and NG. NS: naringenin-4'-*O*-sulfate; NG: naringenin-7-*O*-glucuronide; RLU: relative light unit; I_0/I: fluorescence intensity 0/fluorescence intensity

Note. Reprinted from "Interaction of luteolin, naringenin, and their sulfate and glucuronide conjugates with human serum albumin, cytochrome P450 (CYP2C9, CYP2C19, and CYP3A4) enzymes and organic anion transporting polypeptide (OATP1B1 and OATP2B1) transporters' by Kaci H, Bodnárová S, Fliszár-Nyúl E, Lemli B, Pelantová H, Valentová K, et al. Biomed Pharmacother. 2023;157:114078 (https://doi.org/10.1016/j.biopha.2022.114078). CC BY.

values and the number of binding sites in HSA. Utilizing BMC with polyoxyethylene 23 lauryl ether (Brij-35) as a micellar mobile phase, an *in vitro* system was established to predict the K_b values of food dyes to HSA. A

model was developed to assess the relationship between BMC retention data and the K_b of food dyes, and the predictive capability of the model was evaluated. Moreover, molecular docking studies indicated that synthetic food dyes have the potential to bind within the extensive hydrophobic cavity of site I (subdomain IIA) in HSA [49].

Monascus pigments, secondary metabolites generated by *Monascus* species, have found widespread use as food colorants in China, Japan, Korea, and Southeast Asia for many years. Ankaflavin (AK) stands out as a representative yellow pigment derived from *Monascus*-fermented rice, known for its various biological effects. However, due to its limited solubility, investigations into AK delivery systems, particularly those built from protein-polysaccharide complexes, have garnered significant interest. The study conducted by Wu et al. [50] centered on examining the interactions between AK and BSA, with a specific emphasis on investigating how carrageenan (Car) affects the binding of AK to BSA. Findings indicated that the quenching of BSA by AK occurred through a static quenching mechanism. The resulting BSA-AK complexes were predominantly stabilized by hydrophobic forces, with AK positioned within the hydrophobic cavity of BSA. In contrast to free AK or AK solely complexed with BSA, the BSA-AK-Car complexes exhibited a greater absorption intensity of AK, suggesting alterations in the microenvironment of BSA. This was validated by the rise in the α-helix content of BSA following the creation of BSA-AK-Car complexes. Hydrogen bonding, van der Waals, and electrostatic interactions were identified as the main forces maintaining the BSA-AK-Car complexes. Additionally, the antioxidant activity of *Monascus*-fermented products was adversely affected by BSA, but the introduction of Car could enhance the antioxidant capacity of BSA-*Monascus*-fermented products-Car complexes [50].

Bioallethrin, a commonly used household insecticide, poses a risk of human exposure. Therefore, its cytotoxic effects on human erythrocytes prompted an investigation into its interaction with Hb through both *in silico* and biophysical methods. In the study conducted by Arif et al. [51] when Hb was incubated with increasing concentration of bio-allethrin, an increase in absorbance value was observed, which was accompanied by a slight reduction in the Soret band. Additionally, the intrinsic fluorescence of Hb increased, confirming that a new peak was observed. In this study, synchronous fluorescence analysis suggested that the interaction of bio-allethrin with Hb primarily affected the microenvironment around tyrosine residue. The alterations in Hb structure were validated by a notable shift in CD spectra, accompanied by approximately 25% reduction in α-helical content. Molecular docking, complemented by visualization in Discovery Studio, confirmed the establishment of a Hb-bio-allethrin complex with a binding energy of –7.3 kcal/mol. The structural modifications caused by bio-allethrin resulted in the suppression of the esterase activity of Hb. As a result, this investigation indicates that bio-allethrin establishes a stable complex with human Hb, potentially causing a decline in Hb functionality within the body [51].

Phenolic compounds constitute a vital component of the human diet, garnering interest for their antioxidant properties and potential health benefits. The impact of these compounds on human health is contingent upon consumption levels and bioavailability. Numerous studies have underscored the positive effects of polyphenols on the vascular system, including blood pressure reduction, enhanced endothelial function, bolstered antioxidant defenses, inhibition of platelet aggregation and low-density lipoprotein oxidation, as well as diminished inflammatory responses. Despite several reports highlighting the health benefits of moderate wine consumption, the specific contribution of the primary phenolics in red wine to the quenching properties of major human serum proteins remains unexplored. Shafreen et al. [52] aim to investigate red wine samples for their antioxidant activities, bioactive compounds, and interactions between wine polyphenols and key serum proteins. In this research, the interactions of fibrinogen and HSA with compounds including epicatechin, epigallocatechin, resveratrol, rutin, quercetin, gallic acid, tannic acid, myricetin, CA were examined in detail. As per the findings from fluorescence and molecular docking analyses (Figure 5), tannic acid demonstrated the highest binding affinity with HSA at –10.4 kcal/mol, succeeded by routine with a binding affinity of –9.9 kcal/mol. Additionally, nearly all compounds present in the investigated wine showcased interactions with HSA, as evidenced [52].
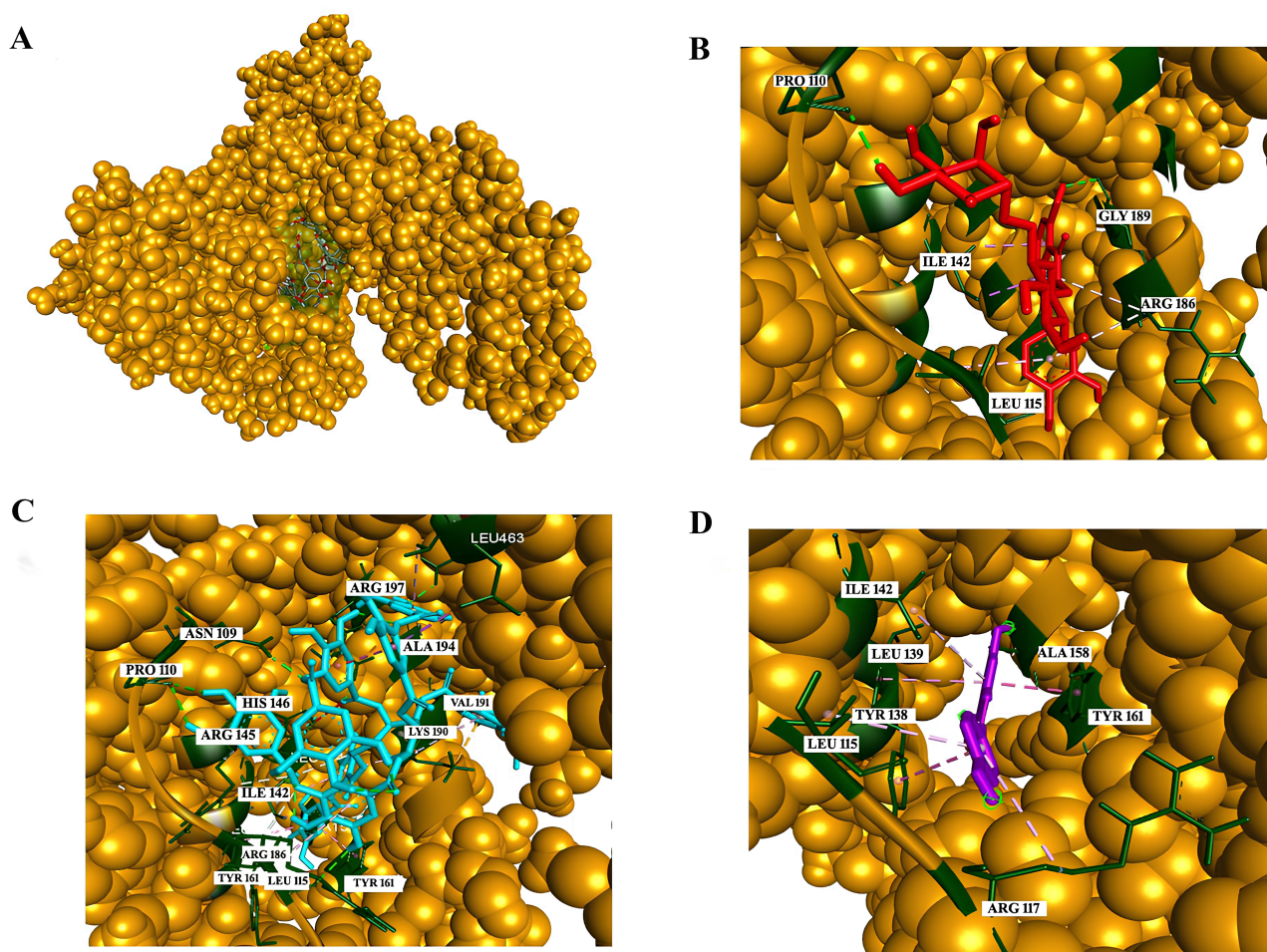
Figure 5. Analysis of interactions with HSA. (A) The green-colored surface represents the binding pocket of the HSA protein [Corey-Pauling-Koltun (CPK) model]; (B) interaction of rutin with the amino acids in the binding pocket; (C) interaction of tannic acid with the amino acids in the binding pocket; (D) interaction of resveratrol with the amino acids in the binding pocket. PRO: proline; ILE: isoleucine; GLY: glycine; ARG: arginine; LEU: leucine; ALA: alanine; VAL: valine; LYS: lysine; TYR: tyrosinase; HIS: histidine; ASN: asparagine

Note. Reprinted from "*In vitro* and *in silico* interaction studies with red wine polyphenols against different proteins from human serum[†]," by Shafreen RMB, Lakshmi SA, Pandian SK, Kim YM, Deutsch J, Katrich E, et al. Molecules. 2021;26:6686 (https://doi.org/10.3390/molecules26216686). CC BY.

Various spectroscopic and computational methods play a pivotal role in elucidating the interactions between serum proteins and environmental compounds like food additives, pesticides, and pollutants. UV-Vis spectroscopy offers advantages in its simplicity and rapid data acquisition, allowing for the assessment of protein structural changes. Fluorescence spectroscopy, with its high sensitivity, provides detailed information on protein conformation alterations and binding affinities. CD spectroscopy is valuable for probing changes in protein secondary structure, although it has limitations in providing precise quantitative data. FTIR spectroscopy allows for the investigation of molecular vibrations and structural modifications in proteins, although it might lack the sensitivity observed in other methods. Molecular docking, a computational tool, is advantageous for predicting binding modes, binding energies, and affinities but is reliant on accurate structural information and may oversimplify the dynamic nature of protein interactions. Combining these techniques offers a multi-faceted understanding of the intricate interactions between serum proteins and various environmental substances, contributing to a comprehensive assessment of their potential physiological effects. Moreover, chromatographic methods are particularly valuable for their ability to separate and quantify individual components in complex mixtures, allowing for the identification of protein-bound contaminants and the assessment of binding affinities. Size-exclusion chromatography (SEC) within high-pressure liquid chromatography (HPLC) is specifically effective in studying changes in protein conformation and interactions. Moreover, gas chromatography is well-suited for volatile compounds, offering high sensitivity in the analysis of pesticide-protein interactions.

While UV-Vis, fluorescence spectroscopy, CD, FTIR, and molecular docking offer valuable information, chromatographic methods significantly contribute to the analytical toolbox for a comprehensive understanding of serum protein interactions with environmental contaminants. To sum up, while these methods collectively offer a comprehensive understanding, it is crucial to recognize the specific strengths and limitations of each technique to draw meaningful conclusions about the intricate interactions between serum proteins and environmental substances.

Within the scope of this review, the interactions of various food additives, pesticides, and contaminants with different serum proteins were examined. Examples of selected studies carried out on this subject since 2020 were presented to researchers. The methods, quenching mechanism, quenching/binding constant, thermodynamic results, and binding region used in these studies were tabulated in detailed (Table 1)

Table 1. Interaction studies with various food additives, pesticides, and contaminants against different serum proteins.

Compound	Protein	Methods	Quenching mechanism	Quenching/ Binding constant	Thermodynamic results	Binding region	Reference
Amaranth	HSA	UV-Vis, fluorescence spectroscopy, CD, molecular docking, and molecular dynamics simulations (MDS)	Static	K_{SV}: 2.78×10^4–3.76×10^4 M^{-1}	$\Delta G° < 0$ (spontaneous) $\Delta H° = -11.8$ kJ/mol $\Delta S° = 0.047$ kJ·mol^{-1}·K^{-1})	Subdomain IIA (site I)	[53]
New coccin	HSA			K_{SV}: 4.1×10^4–5.53×10^4 M^{-1}	$\Delta G° < 0$ (spontaneous) $\Delta H° = -11.7$ kJ/mol $\Delta S° = 0.050$ kJ·mol^{-1}·K^{-1} (Hydrogen bonding and electrostatic forces)		
Myricitrin	HSA	UV-Vis, fluorescence spectroscopy, CD, micro-FTIR, molecular docking, and MDS	Static	K_{SV}: 4.73×10^4–5.76×10^4 M^{-1} K_a: 0.5×10^5 –3.48×10^5 M^{-1}	$\Delta G° < 0$ (spontaneous) $\Delta H° = -16.23$ kJ/mol $\Delta S° = 0.049$ kJ·mol^{-1}·K^{-1} (Hydrogen bonding, hydrophobic interactions, and electrostatic forces)	Subdomain IIA (site I)	[54]
Sodium tripolyphosphate	BSA	UV-Vis, fluorescence spectroscopy, FTIR, and molecular docking	Static	K_{SV}: 4.5×10^3–9.38×10^3 M^{-1} K_a: 4.25×10^1 –2.23×10^6 M^{-1}	$\Delta G° < 0$ (spontaneous) $\Delta H° = -341.3$ kJ/mol $\Delta S° = -1.064$ kJ·mol^{-1}·K^{-1} (Hydrogen bonding and van der Waals forces)	Subdomain IIA (Sudlow's site I)	[55]
2,4,6-Trichlorophenol	BSA	UV-Vis, fluorescence spectroscopy, ITC, and molecular docking	Static	K_{SV}: 1.018×10^6–1.692×10^6 M^{-1} K_a: 1.962×10^5–5.701×10^5 M^{-1}	$\Delta G° < 0$ (spontaneous) $\Delta H° = -58.06$ kJ/mol $\Delta S° = -85.67$ J·mol^{-1}·K^{-1} (Hydrogen bonding and van der Waals forces)	Subdomain IIIA (site II)	[56]
2,4,6-Tribromophenol				K_{SV}: 1.597×10^6–2.941×10^6 M^{-1} K_a: $2.501 \times$	$\Delta G° < 0$ (spontaneous) $\Delta H° = -98.97$ kJ/mol		

Compound	Protein	Methods	Quenching mechanism	Quenching/ Binding constant	Thermodynamic results	Binding region	Reference
				10^5–15.385 $\times 10^5$ M^{-1}	$\Delta S° = -215.76$ J·mol^{-1}·K^{-1} (Hydrogen bonding and van der Waals forces)		
Sodium hydrosulfite	BSA	UV-Vis, fluorescence spectroscopy, FTIR, molecular docking, and surface plasmon resonance (SPR)	Static and dynamic	K_{SV}: 5.13 × 10^3–6.12 × 10^3 M^{-1} K_a: 0.313 × 10^2–44.545 × 10^2 M^{-1}	$\Delta G° < 0$ (spontaneous) $\Delta H° = -139{,}783$ kJ/mol $\Delta S° = -404.592$ J·mol^{-1}·K^{-1} (Hydrogen bonding and van der Waals forces)	Subdomains IIA and IIIA (sites I and II)	[57]
Natamycin	BSA	UV-Vis, fluorescence spectroscopy, molecular docking, and SPR	Static and dynamic	K_{SV}: 5.32 × 10^3–10.01 × 10^3 M^{-1} K_a: 2.13 × 10^2–18.73 × 10^2 M^{-1}	$\Delta G° < 0$ (spontaneous) $\Delta H° = -87.16$ kJ/mol $\Delta S° = -237.6$ J·mol^{-1}·K^{-1} (Hydrogen bonding and van der Waals forces)	Subdomain IIIA (Sudlow's site I)	[58]
Sunset yellow	HSA	UV-Vis, fluorescence spectroscopy, and molecular docking	Static	K_{SV}: 5.15 × 10^4–6.8 × 10^4 M^{-1} K_a: 0.2 × 10^6 –3.11 × 10^6 M^{-1}	$\Delta G° < 0$ (spontaneous) $\Delta H° = -52.24$ kJ/mol $\Delta S° = -50.07$ J·mol^{-1}·K^{-1} (Hydrogen bonding and van der Waals forces)	Sudlow's site I	[59]
Allura red				K_{SV}: 3.75 × 10^4–4.21 × 10^4 M^{-1} K_a: 0.04 × 10^6–0.3 × 10^6 M^{-1}	$\Delta G° < 0$ (spontaneous) $\Delta H° = -58.79$ kJ/mol $\Delta S° = -115.1$ J·mol^{-1}·K^{-1} (Hydrogen bonding and van der Waals forces)		
Propazine	BSA	UV-Vis, fluorescence spectroscopy, and molecular docking	Static	K_{SV}: 1.46 × 10^3–1.60 × 10^3 M^{-1} K_a: 0.6 × 10^{-3}–9.55 × 10^{-3} M^{-1}	$\Delta G° < 0$ (spontaneous) $\Delta H° = -103.45$ kJ/mol $\Delta S° = -0.05$ kJ·mol^{-1}·K^{-1} (Hydrogen bonding, hydrophobic interactions, and van der Waals forces)	Subdomains IIA and IIIA (sites I and II)	[60]
Quinoxyfen				K_{SV}: 4.17 × 10^3–6.39 × 10^3 M^{-1} K_a: 5.01 × 10^2–7.08 × 10^2 M^{-1}	$\Delta G° < 0$ (spontaneous) $\Delta H° = -12.84$ kJ/mol $\Delta S° = 0.01$ kJ·mol^{-1}·K^{-1} (Hydrogen bonding, hydrophobic interactions, and van der Waals forces)		

Table 1. Interaction studies with various food additives, pesticides, and contaminants against different serum proteins. (*continued*)

Compound	Protein	Methods	Quenching mechanism	Quenching/ Binding constant	Thermodynamic results	Binding region	Reference
Aclonifen	HSA	UV-Vis, fluorescence spectroscopy, and molecular docking	Dynamic	K_{SV}: 1.62×10^5–3.05×10^5 M^{-1} K_a: 0.0174×10^6–1.95×10^6 M^{-1}	$\Delta G° < 0$ (spontaneous) $\Delta H° = 225.43$ kJ/mol $\Delta S° = 0.864$ kJ·mol^{-1}·K^{-1} (Hydrophobic interactions)	Subdomains IIA and IIIA (sites I and II)	[61]
Bifenox				K_{SV}: 1.6×10^5–2.10×10^5 M^{-1} K_a: 0.002×10^6–1.02×10^6 M^{-1}	$\Delta G° < 0$ (spontaneous) $\Delta H° = 304.63$ kJ/mol $\Delta S° = 1.11$ kJ·mol^{-1}·K^{-1} (Hydrophobic interactions)		
Phosmet	Bovine hemoglobin (BHb)	UV-Vis, fluorescence spectroscopy, CD, FRET, and molecular docking	Dynamic	K_{SV}: 3.5×10^{-6}–4.8×10^{-6} M^{-1} K_a: 0.004×10^3–6.4×10^3 M^{-1}	$\Delta G° < 0$ (spontaneous) $\Delta H° = -284.97$ kJ/mol $\Delta S° = -88.29$ J·mol^{-1}·K^{-1} (Hydrogen bonding, and van der Waals forces)	NS	[62]
Isoflucypram	HSA	UV-Vis, fluorescence spectroscopy, CD, FTIR, molecular docking, and MDS	Static and dynamic	K_{SV}: 1.593×10^4–1.832×10^4 M^{-1} K_a: 0.158×10^3–4.923×10^3 M^{-1}	$\Delta G° < 0$ (spontaneous) $\Delta H° = -187.549$ kJ/mol $\Delta S° = -563.59$ J·mol^{-1}·K^{-1} (Hydrogen bonding, and van der Waals forces)	Sudlow's site I	[63]
Cuminaldehyde (4-isopropyl benzaldehyde)	HSA	UV-Vis, fluorescence spectroscopy, CD, and molecular docking	Static	K_{SV}: 5.5×10^3–8.3×10^3 M^{-1}	$\Delta G° < 0$ (spontaneous) $\Delta H° = -16.0$ kJ/mol $\Delta S° = 21.6$ J·mol^{-1}·K^{-1} (Hydrophobic forces, and hydrogen bonding)	Subdomain IIA (site I)	[64]
Cuminol (4-isopropyl benzyl alcohol)				K_{SV}: 6.3×10^2–9.4×10^2 M^{-1}	$\Delta G° < 0$ (spontaneous) $\Delta H° = -15.9$ kJ/mol $\Delta S° = 3.3$ J·mol^{-1}·K^{-1} (Hydrophobic forces, and hydrogen bonding)		
Potassium bromate	BSA	UV-Vis, fluorescence spectroscopy, and molecular docking	Static and dynamic	K_{SV}: 1.14×10^4–1.36×10^4 M^{-1} K_a: 9.34×10^3–2.93×10^6 M^{-1}	$\Delta G° < 0$ (spontaneous) $\Delta H° = -122.8$ kJ/mol $\Delta S° = -320.51$ J·mol^{-1}·K^{-1} (Hydrogen bonding, and van der Waals forces)	Subdomain IB (site III)	[65]
Quinoline yellow	Lysozyme	UV-Vis,	Static	K_{SV}: $94.55 \times$	$\Delta G° < 0$	NS	[66]

Table 1. Interaction studies with various food additives, pesticides, and contaminants against different serum proteins. (*continued*)

Compound	Protein	Methods	Quenching mechanism	Quenching/ Binding constant	Thermodynamic results	Binding region	Reference
		fluorescence spectroscopy, CD, molecular docking, and MDS		10^3−125.83 × 10^3 M^{-1} K_a: 5.69 × 10^6−23.76 × 10^6 M^{-1}	(spontaneous) $\Delta H° = -49.02$ kJ/mol $\Delta S° = -32.69$ J·mol^{-1}·K^{-1} (Hydrogen bonding, and van der Waals forces)		
Carbofuran	BSA	UV-Vis, fluorescence spectroscopy, CD, and molecular docking	Static	K_{SV}: 2.02 × 10^4 M^{-1} K_a: 1.17 × 10^8 M^{-1}	NS	Site I	[67]
Naringenin	Lysozyme	UV-Vis, fluorescence spectroscopy, CD, molecular docking, and MDS	Static	K_{SV}: 24.28 × 10^3−66.94 × 10^3 M^{-1} K_a: 53.74 × 10^3 −2,803.14 × 10^3 M^{-1}	$\Delta G° < 0$ (spontaneous) $\Delta H° = 259.13$ kJ/mol $\Delta S° = 953.11$ J·mol^{-1}·K^{-1} (Hydrophobic interactions)	Trp 62, Trp 63, and Trp 108	[68]
Azinphos-methyl	BSA	UV-Vis, fluorescence spectroscopy, CD, FTIR, and molecular docking	Dynamic	K_{SV}: 0.6 × 10^4−1.46 × 10^4 M^{-1} K_a: 0.099 × 10^5−0.209 × 10^5 M^{-1}	$\Delta G° < 0$ (spontaneous) $\Delta H° = -133.25$ kJ/mol $\Delta S° = -0.378$ J·mol^{-1}·K^{-1} (Hydrogen bonding, and van der Waals forces)	Subdomain IB (site III)	[69]
Flupyrimin	BSA	UV-Vis, fluorescence spectroscopy, CD, FTIR, and molecular docking	Static	K_{SV}: 1.664 × 10^4−1.921 × 10^4 M^{-1} K_a: 1.579 × 10^5−1.907 × 10^5 M^{-1}	$\Delta G° < 0$ (spontaneous) $\Delta H° = -14.36$ kJ/mol $\Delta S° = 52.95$ J·mol^{-1}·K^{-1} (Hydrophobic forces, and hydrogen bonding)	Subdomain IIIA (site II)	[70]
	HSA			K_{SV}: 1.909 × 10^4−2.361 × 10^4 M^{-1} K_a: 1.706 × 10^5−2.11 × 10^5 M^{-1}	$\Delta G° < 0$ (spontaneous) $\Delta H° = -16.26$ kJ/mol $\Delta S° = 47.31$ J·mol^{-1}·K^{-1} (Hydrophobic forces, and hydrogen bonding)		
Nitenpyram	BSA			K_{SV}: 2.16 × 10^4−2.349 × 10^4 M^{-1} K_a: 1.911 × 10^5−2.108 × 10^5 M^{-1}	$\Delta G° < 0$ (spontaneous) $\Delta H° = -7.51$ kJ/mol $\Delta S° = 76.76$ J·mol^{-1}·K^{-1} (Hydrophobic forces, and hydrogen bonding)		
	HSA			K_{SV}: 2.225 × 10^4−2.519 × 10^4 M^{-1} K_a: 1.994 ×	$\Delta G° < 0$ (spontaneous) $\Delta H° = -12.40$ kJ/mol		

Compound	Protein	Methods	Quenching mechanism	Quenching/ Binding constant	Thermodynamic results	Binding region	Reference
				10^5–2.346×10^5 M^{-1}	$\Delta S° = 61.16$ J·mol^{-1}·K^{-1} (Hydrophobic forces, and hydrogen bonding)		
Formetanate hydrochloride	HSA	Fluorescence and CD spectroscopy, molecular docking, and MDS	Static	K_{sv}: 0.01–0.02 M^{-1}; K_a: 3.75×10^{-5}–5.14×10^{-5} M^{-1}	$\Delta G° < 0$ (spontaneous); $\Delta H° = 13.46$ kJ/mol; $\Delta S° = 0.15$ J·mol^{-1}·K^{-1} (Hydrophobic forces)	Sudlow's site I and site II	[71]
Mancozeb	Hb	UV-Vis, fluorescence spectroscopy, CD, molecular docking, and MDS	Static	K_{sv}: 2.09×10^4–3.27×10^4 M^{-1}; K_a: 1.76×10^4–5.33×10^4 M^{-1}	$\Delta G° < 0$ (spontaneous); $\Delta H° = -10.35$ kcal/mol; $\Delta S° = -0.013$ kcal·mol^{-1}·K^{-1} (Hydrogen bonding, and van der Waals forces)	NS	[72]
Dicofol	HSA	UV-Vis, fluorescence spectroscopy, CD, molecular docking, and MDS	Static	K_{sv}: 0.73×10^5–1.3×10^5 M^{-1}; K_a: 0.82×10^5–2.77×10^5 M^{-1}	$\Delta G° < 0$ (spontaneous); $\Delta H° = -55.35$ kJ/mol; $\Delta S° = -84.7$ J·mol^{-1}·K^{-1} (Hydrogen bonding, and van der Waals forces)	Suldow's site I	[73]
Salicylic acid	BSA	UV-Vis, fluorescence spectroscopy, CD, and molecular docking	Static and dynamic	K_{sv}: 10.26 M^{-1}	NS	Near the Trp-213	[74]
Beauvericin	HSA	UV-Vis, fluorescence spectroscopy, and molecular docking	NS	NS	NS	NS	[75]
Cyclopiazonic acid				logK_{sv}: 4.37; logK_a: 4.38		Sudlow's site I	
Sterigmatocystin				logK_{sv}: 4.32; logK_a: 3.98		NS	
Butylated hydroxyanisole	BSA	UV-Vis, fluorescence spectroscopy, and molecular docking	Static	K_{sv}: 5.96×10^3–9.3×10^3 M^{-1}; K_a: 0.57×10^4–3.18×10^4 M^{-1}	$\Delta G° < 0$ (spontaneous); $\Delta H° = 110.8$ kJ/mol; $\Delta S° = 443.3$ J·mol^{-1}·K^{-1} (Hydrophobic forces)	Subdomain IIA (site I)	[76]
Sorbic acid	HSA	UV-Vis, fluorescence spectroscopy, CD, FTIR, molecular docking, and MDS	Static	K_{sv}: 5.555×10^4–6.218×10^4 M^{-1}; K_a: 4.033×10^5–5.046×10^5 M^{-1}	$\Delta G° < 0$ (spontaneous); $\Delta H° = -29.366$ kJ/mol; $\Delta S° = 108.149$ J·mol^{-1}·K^{-1} (Hydrogen bonding, and hydrophobic forces)	Subdomain IIA (site I)	[77]
Dicyclohexyl phthalate	HSA	UV-Vis, fluorescence spectroscopy, CD, FTIR, and	Static	K_{sv}: 2.05×10^5 M^{-1}; K_a: $13.47 \times$	$\Delta G° < 0$ *(spontaneous)*; $\Delta H° = -39.26$ kJ/mol	Subdomain IIA (site I)	[78]

Compound	Protein	Methods	Quenching mechanism	Quenching/ Binding constant	Thermodynamic results	Binding region	Reference
		molecular docking		10^4−39.54 × 10^4 M^{-1}	$\Delta S° = -29.14$ J·mol^{-1}·K^{-1}		
					(Hydrogen bonding, and van der Waals forces)		
Monocyclohexyl phthalate				K_{SV}: 1.24 × 10^5 M^{-1}	$\Delta G° < 0$ (spontaneous)		
				K_a: 0.7 × 10^4 −1.72 × 10^4 M^{-1}	$\Delta H° = -43.18$ kJ/mol		
					$\Delta S° = -68.34$ J·mol^{-1}·K^{-1}		
					(Hydrogen bonding, and van der Waals forces)		
Malachite green oxalate	HSA	UV-Vis, fluorescence spectroscopy, CD, molecular docking, and MDS	Static	K_{SV}: 374.9 M^{-1}	$\Delta G° < 0$ (spontaneous)	NS	[79]
				K_a: 4.35 × 10^6 M^{-1}	(Hydrogen bonding, and van der Waals forces)		
Lutein dipalmitate	BSA	UV-Vis, fluorescence spectroscopy, CD, and molecular docking	Dynamic	K_{SV}: 2.17 × 10^4 −3.22 × 10^4 M^{-1}	$\Delta G° < 0$ (spontaneous)	Subdomain IIA (site I)	[80]
				K_a: 0.63 × 10^4 −2.75 × 10^4 M^{-1}	$\Delta H° = -56.82$ kJ/mol		
					$\Delta S° = -106.02$ J·mol^{-1}·K^{-1}		
					(Hydrogen bonding, and van der Waals forces)		
Chlorpyrifos	α_2M	UV-Vis, fluorescence spectroscopy, CD, and molecular docking	Static	K_{SV}: 1.017 × 10^4 −1.656 × 10^4 M^{-1}	$\Delta G° < 0$ (spontaneous)	Receptor-binding domain of the α_2M	[81]
				K_a: 5.432 × 10^{-4} −6.181 × 10^{-4} M^{-1}	$\Delta H° = 15.62$ kJ/mol		
					$\Delta S° = 60.25$ J·mol^{-1}·K^{-1}		
					(Hydrophobic forces)		
Epoxiconazole	BSA	UV-Vis, fluorescence spectroscopy, CD, and molecular docking	Static	K_a: 0.79 × 10^4 −3.8 × 10^4 M^{-1}	$\Delta G° < 0$ (spontaneous)	Subdomain IIA (site I)	[82]
					$\Delta H° = -81.54$ kJ/mol		
					$\Delta S° = -199.35$ J·mol^{-1}·K^{-1}		
					(Hydrogen bonding, and van der Waals forces)		
	HSA			K_a: 0.814 × 10^4 −6.22 × 10^4 M^{-1}	$\Delta G° < 0$ (spontaneous)		
					$\Delta H° = -105.74$ kJ/mol		
					$\Delta S° = -265.88$ J·mol^{-1}·K^{-1}		
					(Hydrogen bonding, and van der Waals forces)		
Prothioconazole	BSA			K_a: 1.66 × 10^5 −6.45 × 10^5 M^{-1}	$\Delta G° < 0$ (spontaneous)		
					$\Delta H° = -84.85$ kJ/mol		
					$\Delta S° = -174.18$ J·mol^{-1}·K^{-1}		
					(Hydrogen bonding, and van der Waals		

Compound	Protein	Methods	Quenching mechanism	Quenching/ Binding constant	Thermodynamic results	Binding region	Reference
	HSA			K_a: 2.08 × 10^5−5.75 × 10^5 M^{-1}	ΔG° < 0 (spontaneous) ΔH° = −64.39 kJ/mol ΔS° = −105.50 J·mol^{-1}·K^{-1} (Hydrogen bonding, and van der Waals forces)		
Dicofol	HSA	UV-Vis, fluorescence spectroscopy, CD, ITC, and molecular docking	Static	K_{SV}: 1.18 × 10^4−1.37 × 10^4 M^{-1} K_a: 4.38 × 10^4 M^{-1}	ΔG° < 0 (spontaneous) ΔH° = −5.42 kJ/mol ΔS° = 21.08 J·mol^{-1}·K^{-1} (Hydrogen bonding, and hydrophobic forces)	Subdomain IIA (site I)	[83]
Thiamethoxam	Lysozyme	UV-Vis, fluorescence spectroscopy, molecular docking, and MDS	Static	K_{SV}: 0.2 × 10^4−0.25 × 10^4 M^{-1} K_a: 0.12 × 10^4−0.45 × 10^4 M^{-1}	ΔG° < 0 (spontaneous) ΔH° = 58.5 kJ/mol ΔS° = 372.55 J·mol^{-1}·K^{-1} (Hydrophobic interactions)	NS	[84]
	BSA			K_{SV}: 1.1 × 10^4−1.15 × 10^4 M^{-1} K_a: 1.93 × 10^4−4.99 × 10^4 M^{-1}	ΔG° < 0 (spontaneous) ΔH° = 11.94 kJ/mol ΔS° = 231.88 J·mol^{-1}·K^{-1} (Hydrophobic interactions)	Site I	
	HSA			K_{SV}: 1.24 × 10^4−1.35 × 10^4 M^{-1} K_a: 1.91 × 10^4−2.41 × 10^4 M^{-1}	ΔG° < 0 (spontaneous) ΔH° = 12.84 kJ/mol ΔS° = 235.20 J·mol^{-1}·K^{-1} (Hydrophobic interactions)		
Phosmet	BSA	UV-Vis, fluorescence spectroscopy, CD, and molecular docking	Static	K_a: 0.15 × 10^4−3.68 × 10^4 M^{-1}	ΔG° < 0 (spontaneous) ΔH° = −16.33 kJ/mol ΔS° = −469 kJ·mol^{-1}·K^{-1} (Hydrogen bonding, and van der Waals forces)	Sudlow's site II	[85]
Phosmet	Lysozyme	UV-Vis, fluorescence spectroscopy, CD, FTIR, and molecular docking	Static	K_{SV}: 0.42 × 10^4−1.51 × 10^4 M^{-1} K_a: 0.0168 × 10^4−9.14 × 10^4 M^{-1}	ΔG° < 0 (spontaneous) ΔH° = −60.2 kJ/mol ΔS° = −187.78 J·mol^{-1}·K^{-1} (Hydrogen bonding, and van der Waals forces)	NS	[86]

Table 1. Interaction studies with various food additives, pesticides, and contaminants against different serum proteins. (*continued*)

Compound	Protein	Methods	Quenching mechanism	Quenching/ Binding constant	Thermodynamic results	Binding region	Reference
β-Resorcylic acid	Lysozyme	UV-Vis, fluorescence spectroscopy, CD, FRET, and molecular docking	Static	K_{SV}: 1.69 × 10^3–5.15 × 10^3 M^{-1} K_a: 1.13 × 10^3–4.68×10^3 M^{-1}	$\Delta G° < 0$ (spontaneous) $\Delta H° = -13.97$ kcal/mol $\Delta S° = -29.42$ cal·mol^{-1}·K^{-1} (Hydrogen bonding, and van der Waals forces)	Amino acid residues: Arg115, Arg119, Try124, and Gln123	[87]
Acenaphthene	BSA	UV-Vis, fluorescence spectroscopy, CD, FTIR, and molecular docking	Static	K_{SV}: 1.98 × 10^5 M^{-1} K_a: 3.82 × 10^5 M^{-1}	NS	Subdomain IB (site III)	[88]
Quinoline yellow	αLA	UV-Vis, fluorescence spectroscopy, CD, molecular docking, and MDS	Dynamic	K_{SV}: 4.0 × 10^{-4}–4.4 × 10^{-4} M^{-1} K_a: 0.091 × 10^{-5}–0.955 × 10^{-5} M^{-1}	$\Delta G° < 0$ (spontaneous) $\Delta H° = 18.79$ kcal/mol $\Delta S° = 83.71$ cal·mol^{-1}·K^{-1} (Hydrophobic interactions)	Central binding site of αLA	[89]
Monosodium glutamate	BSA	UV-Vis, fluorescence spectroscopy, CD, molecular docking, and MDS	Static and dynamic	K_{SV}: 1.873 × 10^3–2.836 × 10^3 M^{-1} K_a: 1.151 × 10^1–4.05 × 10^4 M^{-1}	$\Delta G° < 0$ (spontaneous) $\Delta H° = 243.903$ kJ/mol $\Delta S° = 888.291$ J·mol^{-1}·K^{-1} (Hydrophobic interactions)	Sudlow's site II	[90]
Calcium lactate	BSA	UV-Vis, fluorescence spectroscopy, CD, and molecular docking	Static and dynamic	K_{SV}: 2.06 × 10^3–3.21 × 10^3 M^{-1} K_a: 1.44 × 10^2–2.9 × 10^2 M^{-1}	$\Delta G° < 0$ (spontaneous) $\Delta H° = -7.493$ kJ/mol $\Delta S° = 24.61$ J·mol^{-1}·K^{-1} (Electrostatic forces)	Sudlow's site II (subdomain IIIA)	[91]
Sudan III	BSA	UV-Vis, fluorescence spectroscopy, CD, and molecular docking	Static	K_a: 5.83 × 10^2–6.41 × 10^2 M^{-1}	$\Delta G° < 0$ (spontaneous) $\Delta H° = -5.65$ kJ/mol $\Delta S° = 53.8$ J·mol^{-1}·K^{-1} (Hydrogen bonding, and van der Waals forces)	Subdomain IIA (site I)	[92]
Rhodamine B	HSA	UV-Vis, fluorescence spectroscopy, CD, FTIR, nuclear magnetic resonance (NMR), and molecular docking	Static	K_{SV}: 5.86 × 10^4–6.23 × 10^4 M^{-1} K_a: 6.06 × 10^4–6.35 × 10^4 M^{-1}	$\Delta G° < 0$ (spontaneous) $\Delta H° = -2.99$ kJ/mol $\Delta S° = 81.91$ J·mol^{-1}·K^{-1} (Electrostatic forces)	Subdomain IIA (site I)	[93]
Rosmarinic acid	HSA	UV-Vis, fluorescence spectroscopy, CD, ITC, molecular docking, and MDS	Static	K_{SV}: 1.5 × 10^4–2.7 × 10^4 M^{-1} K_a: 0.36 × 10^7–1.1 × 10^7 M^{-1}	$\Delta G° < 0$ (spontaneous) $\Delta H° = 11.7016$ kcal/mol $\Delta S° = 71.1303$ cal·mol^{-1}·K^{-1} (Hydrophobic forces)	NS	[94]

Table 1. Interaction studies with various food additives, pesticides, and contaminants against different serum proteins. (*continued*)

Compound	Protein	Methods	Quenching mechanism	Quenching/ Binding constant	Thermodynamic results	Binding region	Reference
5-Hydroxymethyl-2-furaldehyde	HSA	UV-Vis, fluorescence spectroscopy, CD, and molecular docking	Static	K_{sv}: 3.25 × 10^4–4.91 × 10^4 M^{-1} K_a: 3.72 × 10^4–5.25 × 10^4 M^{-1}	ΔG° < 0 (spontaneous) ΔH° = −30.02 kJ/mol ΔS° = −10.14 J/·mol^{-1}·K^{-1} (Hydrogen bonding, and van der Waals forces)	Subdomain IIA (site I)	[95]
3,5,6-Trichloro-2-pyridinol	BSA	Fluorescence spectroscopy, NMR, and molecular docking	Static	K_{sv}: 2.1 × 10^5 M^{-1}	ΔG° < 0 (spontaneous) ΔH° = 23.77 kJ/mol ΔS° = 146.98 J·mol^{-1}·K^{-1} (Hydrophobic forces)	Subdomain IIA (site I)	[96]
Paraoxon methyl				K_{sv}: 4.09 × 10^4 M^{-1}	ΔG° < 0 (spontaneous) ΔH° = 94.74 kJ/mol ΔS° = 372.93 J·mol^{-1}·K^{-1} (Hydrophobic forces)	Subdomain IIA and IIIA (sites I and II)	
Chlorpyrifos	HSA	Solid-phase microextraction (SPME), and molecular docking	NS	K_a: 1.42 × 10^5 M^{-1}	NS	NS	[97]
Parathion-methyl				K_a: 1.45 × 10^4–8.19 × 10^4 M^{-1}	ΔG° < 0 (spontaneous) ΔH° = −193.3 kJ/mol ΔS° = −543.7 J·mol^{-1}·K^{-1} (Hydrogen bonding, and van der Waals forces)	Subdomain IIA (site I)	
Malathion				K_a: 1.07 × 10^4–4.02 × 10^4 M^{-1}	ΔG° < 0 (spontaneous) ΔH° = −147.7 kJ/mol ΔS° = −399.2 J·mol^{-1}·K^{-1} (Hydrogen bonding, and van der Waals forces)	Subdomain IIIA (site II)	
Benthiavalicarb-isopropyl	HSA	UV-Vis, fluorescence spectroscopy, CD, molecular docking, and MDS	Static	K_{sv}: 4.41 × 10^3–8.66 × 10^3 M^{-1} K_a: 0.032 × 10^2–7.965 × 10^2 M^{-1}	ΔG° < 0 (spontaneous) ΔH° = −206.39 kJ/mol ΔS° = −654.93 J·mol^{-1}·K^{-1} (Hydrogen bonding, and van der Waals forces)	Hydrophobic cavity of HSA	[98]
Pendimethalin	HSA	UV-Vis, fluorescence spectroscopy, CD, molecular docking, and MDS	Static	K_{sv}: 7.17 × 10^4–9.92 × 10^4 M^{-1} K_a: 8.47 × 10^4–10.63 × 10^4 M^{-1}	ΔG° < 0 (spontaneous) ΔH° = −16.17 kJ/mol ΔS° = 45.78 J·mol^{-1}·K^{-1} (Hydrophobic forces)	Subdomain IIA (Sudlow's site I)	[99]
Tebuconazole	BSA	UV-Vis, fluorescence	Static	K_a: 2.25 × 10^2–4.67 ×	ΔG° < 0	NS	[100]

Table 1. Interaction studies with various food additives, pesticides, and contaminants against different serum proteins. (*continued*)

Compound	Protein	Methods	Quenching mechanism	Quenching/ Binding constant	Thermodynamic results	Binding region	Reference
		spectroscopy, and CD		10^2 M^{-1}	(spontaneous)		
					$\Delta H° = -46.72$ kJ/mol		
					$\Delta S° = -105.67$ J·mol^{-1}·K^{-1}		
					(Hydrogen bonding, and van der Waals forces)		
Perfluorooctanoic acid	HSA	UV-Vis, fluorescence spectroscopy, FTIR, and molecular docking	Static	K_{sv}: 1.076×10^4–1.328×10^4 M^{-1} K_a: 0.4463×10^4–0.6153×10^4 M^{-1}	$\Delta G° < 0$ (spontaneous) $\Delta H° = -17.48$ kJ/mol $\Delta S° = 13.53$ J·mol^{-1}·K^{-1} (Electrostatic forces)	Site I	[101]
Perfluorodecanoic acid				K_{sv}: 1.431×10^4–1.731×10^4 M^{-1} K_a: 1.4514×10^4–2.6788×10^4 M^{-1}	$\Delta G° < 0$ (spontaneous) $\Delta H° = -33.37$ kJ/mol $\Delta S° = -27.91$ J·mol^{-1}·K^{-1} (Hydrogen bonding, and van der Waals forces)		
Acesulfame	HSA	UV-Vis, fluorescence spectroscopy, CD, and molecular docking	Static	K_{sv}: 0.81×10^3–1.77×10^3 M^{-1} K_a: 1.74×10^2–1.82×10^2 M^{-1}	$\Delta G° < 0$ (spontaneous) $\Delta H° = -2.88$ kJ/mol $\Delta S° = 33.66$ J·mol^{-1}·K^{-1} (Electrostatic forces)	Subdomain IIA (site I)	[102]

K_{sv} is Stern-Volmer or quenching constant. K_a is binding constant. $\Delta G°$: Gibbs free energy change; $\Delta H°$: enthalpy change; $\Delta S°$: entropy change. α_2M: alpha-2-macroglobulin; αLA: alpha-lactalbumin; NS: not stated

Conclusions

In recent years, the surge in published articles dedicated to protein-ligand interactions has been significant, thanks to the integration of diverse analytical, and computational techniques in research. These studies utilize various methods to validate the interaction and binding modes of both novel and established ligands with proteins, offering valuable insights into their mechanisms of action. This review presents a comprehensive overview of commonly employed techniques in this field and their interaction applications of various food additives, pesticides, and contaminants with serum proteins.

Abbreviations

3-PBA: 3-phenoxybenzoic acid

4-F-3-PBA: 4-fluoro-3-phenoxybenzoic acid

AK: ankaflavin

BMC: biopartitioning micellar chromatography

BSA: bovine serum albumin

C3G: cyandin-3-*O*-glucoside

CA: caffeic acid

Car: carrageenan

CD: circular dichroism

CHA: chlorogenic acid

FRET: Förster (fluorescence) resonance energy transfer

FTIR: Fourier transform infrared

Hb: human hemoglobin

HSA: human serum albumin

ITC: isothermal titration calorimetry

MD: molecular dynamics

MDS: molecular dynamics simulations

Trp: tryptophan

UV-Vis: Ultraviolet-visible

Declarations

Author contributions

CE and MZK: Conceptualization, Investigation, Writing—original draft, Writing—review & editing.

Conflicts of interest

Cem Erkmen is the GE of Exploration of Foods and Foodomics, but he had no involvement in the journal review process of this manuscript. Both authors declare that they have no conflicts of interest.

Ethical approval

Not applicable.

Consent to participate

Not applicable.

Consent to publication

Not applicable.

Availability of data and materials

Not applicable.

Funding

Not applicable.

Copyright

References

1. Rathi BS, Kumar PS, Vo DVN. Critical review on hazardous pollutants in water environment: occurrence, monitoring, fate, removal technologies and risk assessment. Sci Total Environ. 2021; 797:149134.
2. Rathi BS, Kumar PS, Show PL. A review on effective removal of emerging contaminants from aquatic systems: current trends and scope for further research. J Hazard Mater. 2021;409:124413.
3. Mostafalou S, Abdollahi M. Pesticides and human chronic diseases: evidences, mechanisms, and perspectives. Toxicol Appl Pharmacol. 2013;268:157–77.

4.   Ali H, Khan E, Ilahi I. Environmental chemistry and ecotoxicology of hazardous heavy metals: environmental persistence, toxicity, and bioaccumulation. J Chem. 2019;2019:6730305.

5.   Kim KH, Kabir E, Jahan SA. Exposure to pesticides and the associated human health effects. Sci Total Environ. 2017;575:525–35.

6.   Foong SY, Ma NL, Lam SS, Peng W, Low F, Lee BHK, et al. A recent global review of hazardous chlorpyrifos pesticide in fruit and vegetables: prevalence, remediation and actions needed. J Hazard Mater. 2020;400:123006.

7.   Xiong RG, Li J, Cheng J, Wu SX, Huang SY, Zhou DD, et al. New insights into the protection of dietary components on anxiety, depression, and other mental disorders caused by contaminants and food additives. Trends Food Sci Technol. 2023;138:44–56.

8.   Kaur I, Batra V, Kumar Reddy Bogireddy N, Torres Landa SD, Agarwal V. Detection of organic pollutants, food additives and antibiotics using sustainable carbon dots. Food Chem. 2023;406: 135029.

9.   Khalid AS, Niaz T, Zarif B, Shabbir S, Noor T, Shahid R, et al. Milk phospholipids-based nanostructures functionalized with rhamnolipids and bacteriocin: intrinsic and synergistic antimicrobial activity for cheese preservation. Food Biosci. 2022;47:101442.

10. Zarif B, Haris M, Shahid R, Sherazi TA, Rahman A, Noor T, et al. Potential of milk fat globule membrane's phospholipids and anhydrous milk fat based nanostructured lipid carriers for enhanced bioaccessibility of vitamin D_3. Int Dairy J. 2023;147:105766.

11. Guo W, Pan B, Sakkiah S, Yavas G, Ge W, Zou W, et al. Persistent organic pollutants in food: contamination sources, health effects and detection methods. Int J Environ Res Public Health. 2019; 16:4361.

12. Lebelo K, Malebo N, Mochane MJ, Masinde M. Chemical contamination pathways and the food safety implications along the various stages of food production: a review. Int J Environ Res Public Health. 2021;18:5795.

13. Costopoulou D, Vassiliadou I, Leondiadis L. Infant dietary exposure to dioxins and dioxin-like compounds in Greece. Food Chem Toxicol. 2013;59:316–24.

14. van den Berg M, Kypke K, Kotz A, Tritscher A, Lee SY, Magulova K, et al. WHO/UNEP global surveys of PCDDs, PCDFs, PCBs and DDTs in human milk and benefit–risk evaluation of breastfeeding. Arch Toxicol. 2017;91:83–96.

15. Yan X, Yuan D, Pan D. Interactions of bromocarbazoles with human serum albumin using spectroscopic methods. Molecules. 2018;23:3120.

16. Zhang YL, Zhang X, Fei XC, Wang SL, Gao HW. Binding of bisphenol A and acrylamide to BSA and DNA: insights into the comparative interactions of harmful chemicals with functional biomacromolecules. J Hazard Mater. 2010;182:877–85.

17. Abboud R, Charcosset C, Greige-Gerges H. Interaction of triterpenoids with human serum albumin: a review. Chem Phys Lipids. 2017;207:260–70.

18. Xue P, Zhang G, Zhang J, Ren L. Interaction of flavonoids with serum albumin: a review. Curr Protein Pept Sci. 2021;22:217–27.

19. Dixit S, Ahsan H, Khan FH. Pesticides and plasma proteins: unexplored dimensions in neurotoxicity. Int J Pest Manage. 2023;69:278–87.

20. Yang F, Zhang Y, Liang H. Interactive association of drugs binding to human serum albumin. Int J Mol Sci. 2014;15:3580–95.

21. Espósito BP, Najjar R. Interactions of antitumoral platinum-group metallodrugs with albumin. Coord Chem Rev. 2002;232:137–49.

22. Rimac H, Debeljak Ž, Bojić M, Miller L. Displacement of drugs from human serum albumin: from molecular interactions to clinical significance. Curr Med Chem. 2017;24:1930–47.

23. Tu M, Zheng X, Liu P, Wang S, Yan Z, Sun Q, et al. Typical organic pollutant-protein interactions studies through spectroscopy, molecular docking and crystallography: a review. Sci Total Environ. 2021;763:142959.

24. Kratz F. Albumin as a drug carrier: design of prodrugs, drug conjugates and nanoparticles. J Control Release. 2008;132:171–83.

25. He XM, Carter DC. Atomic structure and chemistry of human serum albumin. Nature. 1992;358: 209–15. Erratum in: Nature. 1993;364:362.

26. Majorek KA, Porebski PJ, Dayal A, Zimmerman MD, Jablonska K, Stewart AJ, et al. Structural and immunologic characterization of bovine, horse, and rabbit serum albumins. Mol Immunol. 2012;52: 174–82.

27. Bujacz A. Structures of bovine, equine and leporine serum albumin. Acta Crystallogr Sect D Biol Crystallogr. 2012;68:1278–89.

28. Shahabadi N, Zendehcheshm S, Mahdavi M. Exploring the *in-vitro* antibacterial activity and protein (human serum albumin, human hemoglobin and lysozyme) interaction of hexagonal silver nanoparticle obtained from wood extract of wild cherry shrub. ChemistrySelect. 2023;8: e202204672.

29. Manning JM, Manning LR, Dumoulin A, Padovan JC, Chait B. Embryonic and fetal human hemoglobins: structures, oxygen binding, and physiological roles. In: Hoeger U, Harris J, editors. Vertebrate and Invertebrate Respiratory Proteins, Lipoproteins and other Body Fluid Proteins. Berlin: Springer; 2020. pp. 275–96.

30. Shrake A, Rupley JA. Environment and exposure to solvent of protein atoms. Lysozyme and insulin. J Mol Biol. 1973;79:351–64.

31. Amadei A, Linssen ABM, Berendsen HJC. Essential dynamics of proteins. Proteins. 1993;17:412–25.

32. Siddiqui S, Ameen F, ur Rehman S, Sarwar T, Tabish M. Studying the interaction of drug/ligand with serum albumin. 2021;336:116200.

33. Gao H, Lei L, Liu J, Kong Q, Chen X, Hu Z. The study on the interaction between human serum albumin and a new reagent with antitumour activity by spectrophotometric methods. J Photochem Photobiol A Chem. 2004;167:213–21.

34. Ma W, Yang L, He L. Overview of the detection methods for equilibrium dissociation constant K_D of drug-receptor interaction. J Pharm Anal. 2018;8:147–52.

35. Wang L, Zhang W, Shao Y, Zhang D, Guo G, Wang X. Analytical methods for obtaining binding parameters of drug–protein interactions: a review. Anal Chim Acta. 2022;1219:340012.

36. Teunissen AJP, Pérez-Medina C, Meijerink A, Mulder WJM. Investigating supramolecular systems using Förster resonance energy transfer. Chem Soc Rev. 2018;47:7027–44.

37. Martin SF, Tatham MH, Hay RT, Samuel IDW. Quantitative analysis of multi-protein interactions using FRET: application to the SUMO pathway. Protein Sci. 2008;17:777–84.

38. Greenfield NJ. Circular dichroism analysis for protein-protein interactions. Methods Mol Biol. (Clifton, N.J.). 2004;261:55–78.

39. Pierce MM, Raman CS, Nall BT. Isothermal titration calorimetry of protein-protein interactions. Methods. 1999;19:213–21.

40. Chatterjee T, Pal A, Dey S, Chatterjee BK, Chakrabarti P. Interaction of virstatin with human serum albumin: spectroscopic analysis and molecular modeling. PLoS One. 2012;7:e37468.

41. Rabbani G, Baig MH, Lee EJ, Cho WK, Ma JY, Choi I. Biophysical study on the interaction between eperisone hydrochloride and human serum albumin using spectroscopic, calorimetric, and molecular docking analyses. Mol Pharm. 2017;14:1656–65.

42. Morris CJ, Corte DD. Using molecular docking and molecular dynamics to investigate protein-ligand interactions. Mod Phys Lett B. 2021;35:2130002.

43. Fu Y, Zhao J, Chen Z. Insights into the molecular mechanisms of protein-ligand interactions by molecular docking and molecular dynamics simulation: a case of oligopeptide binding protein. Comput Math Methods Med. 2018;2018:3502514.

44. Filipe HAL, Loura LMS. Molecular dynamics simulations: advances and applications. Molecules. 2022;27:2105.

45. Cui Y, Sun Y, Yu H, Guo Y, Yao W, Xie Y, et al. Exploring the binding mechanism and adverse toxic effects of degradation metabolites of pyrethroid insecticides to human serum albumin: multi-spectroscopy, calorimetric and molecular docking approaches. Food Chem Toxicol. 2023;179: 113951.

46. Yang P, Wang W, Xu Z, Rao L, Zhao L, Wang Y, et al. New insights into the pH dependence of anthocyanin-protein interactions by a case study of cyanidin-3-O-glucoside and bovine serum albumin. Food Hydrocoll. 2023;140:108649.

47. Kaci H, Bodnárová S, Fliszár-Nyúl E, Lemli B, Pelantová H, Valentová K, et al. Interaction of luteolin, naringenin, and their sulfate and glucuronide conjugates with human serum albumin, cytochrome P450 (CYP2C9, CYP2C19, and CYP3A4) enzymes and organic anion transporting polypeptide (OATP1B1 and OATP2B1) transporters. Biomed Pharmacother. 2023;157:114078.

48. Zhang L, Guan Q, Tang L, Jiang J, Sun K, Manirafasha E, et al. Effect of Cu^{2+} and Al^{3+} on the interaction of chlorogenic acid and caffeic acid with serum albumin. Food Chem. 2023;410:135406.

49. Hoseyni P, Fatemi MH, Hadjmohammadi M, Majidi SM. Experimental and theoretical studies of the interactions of some synthetic food dyes with human serum albumin. J Iran Chem Soc. 2022;19: 885–92.

50. Wu S, Wang W, Lu J, Deng W, Zhao N, Sun Y, et al. Binding of ankaflavin with bovine serum albumin (BSA) in the presence of carrageenan and protective effects of *Monascus* yellow pigments against oxidative damage to BSA after forming a complex with carrageenan. Food Funct. 2023;14:2459–71.

51. Arif A, Hashmi MA, Salam S, Younus H, Mahmood R. Interaction of the insecticide bioallethrin with human hemoglobin: biophysical, *in silico* and enzymatic studies. J Biomol Struct Dyn. 2023;41: 6591–602.

52. Shafreen RMB, Lakshmi SA, Pandian SK, Kim YM, Deutsch J, Katrich E, et al. *In vitro* and in silico interaction studies with red wine polyphenols against different proteins from human serum[†]. Molecules. 2021;26:6686.

53. Chaves OA, Loureiro RJS, Costa-Tuna A, Almeida ZL, Pina J, Brito RMM, et al. Interaction of two commercial azobenzene food dyes, amaranth and new coccine, with human serum albumin: biophysical characterization. ACS Food Sci Technol. 2023;3:955–68.

54. Niu T, Zhu X, Zhao D, Li H, Yan P, Zhao L, et al. Unveiling interaction mechanisms between myricitrin and human serum albumin: insights from multi-spectroscopic, molecular docking and molecular dynamic simulation analyses. Spectrochim Acta A Mol Biomol Spectrosc. 2023;285:121871.

55. Esazadeh K, Azimirad M, Yekta R, Ezzati Nazhad Dolatabadi J, Ghanbarzadeh B. Multi-spectroscopies and molecular simulation insights into the binding of bovine serum albumin and sodium tripolyphosphate. J Photochem Photobiol A Chem. 2023;444:114999.

56. Liang W, Zhang Z, Zhu Q, Han Z, Huang C, Liang X, et al. Molecular interactions between bovine serum albumin (BSA) and trihalophenol: insights from spectroscopic, calorimetric and molecular modeling studies. Spectrochim Acta Part A Mol Biomol Spectrosc. 2023;287:122054.

57. Zaheri M, Azimirad M, Yekta R, Ezzati Nazhad Dolatabadi J, Torbati M. Kinetic and thermodynamic aspects on the interaction of serum albumin with sodium hydrosulfite: spectroscopic and molecular docking methods. J Photochem Photobiol A Chem. 2023;442:114804.

58. Azimirad M, Javaheri-Ghezeldizaj F, Yekta R, Ezzati Nazhad Dolatabadi J, Torbati M. Mechanistic and kinetic aspects of Natamycin interaction with serum albumin using spectroscopic and molecular docking methods. Arab J Chem. 2023;16:105043.

59. Wang J, Cheng J. Spectroscopic and molecular docking studies of the interactions of sunset yellow and allura red with human serum albumin. J Food Saf. 2023;43:e13030.

60. Duman B, Erkmen C, Zahirul Kabir M, Ching Yi L, Mohamad SB, Uslu B. *In vitro* interactions of two pesticides, propazine and quinoxyfen with bovine serum albumin: spectrofluorometric and molecular docking investigations. Spectrochim Acta Part A Mol Biomol Spectrosc. 2023;300:122907.

61. Sapmaz H, Erkmen C, Kabır MZ, Tayyab H, Mohamad SB, Uslu B. Spectrofluorometric and computational approaches for the interaction studies of aclonifen and bifenox with human serum albumin. Spectrochim Acta Part A Mol Biomol Spectrosc. 2023;284:121772.

62. Kaur L, Singh A, Datta A, Ojha H. Multispectroscopic studies of binding interaction of phosmet with bovine hemoglobin. Spectrochim Acta Part A Mol Biomol Spectrosc. 2023;296:122630.

63. Li X, Yan X, Yang D, Chen S, Yuan H. Probing the interaction between isoflucypram fungicides and human serum albumin: multiple spectroscopic and molecular modeling investigations. Int J Mol Sci. 2023;24:12521.

64. Ali MS, Rehman MT, Al-Lohedan H, Alajmi MF. Spectroscopic and molecular docking investigation on the interaction of cumin components with plasma protein: assessment of the comparative interactions of aldehyde and alcohol with human serum albumin. Int J Mol Sci. 2022;23:4078.

65. Mahmoudpour M, Karimzadeh Z, Yekta R, Torbati M, Ezzati Nazhad Dolatabadi J. Exploring the binding mode between potassium bromate and bovine serum albumin: multi-spectroscopic and molecular modeling analysis. J Mol Liq. 2022;348:118060.

66. Asemi-Esfahani Z, Shareghi B, Farhadian S, Momeni L. Food additive dye–lysozyme complexation: determination of binding constants and binding sites by fluorescence spectroscopy and modeling methods. J Mol Liq. 2022;363:119749.

67. Nagtilak M, Pawar S, Labade S, Khilare C, Sawant S. Study of the binding interaction between bovine serum albumin and carbofuran insecticide: multispectroscopic and molecular docking techniques. J Mol Struct. 2022;1249:131597.

68. Ashrafi N, Shareghi B, Farhadian S, Hosseini-Koupaei M. A comparative study of the interaction of naringenin with lysozyme by multi-spectroscopic methods, activity comparisons, and molecular modeling procedures. Spectrochim Acta Part A Mol Biomol Spectrosc. 2022;271:120931.

69. Farasati Far B, Asadi S, Naimi-Jamal MR, Abdelbasset WK, Aghajani Shahrivar A. Insights into the interaction of azinphos-methyl with bovine serum albumin: experimental and molecular docking studies. J Biomol Struct Dyn. 2022;40:11863–73.

70. Zhao Z, Shi T, Chu Y, Cao Y, Cheng S, Na R, et al. Comparison of the interactions of flupyrimin and nitenpyram with serum albumins via multiple analysis methods. Chemosphere. 2022;289:133139.

71. Singh S, Gopi P, Pandya P. Structural aspects of formetanate hydrochloride binding with human serum albumin using spectroscopic and molecular modeling techniques. Spectrochim Acta Part A Mol Biomol Spectrosc. 2022;281:121618.

72. Quds R, Amiruddin Hashmi M, Iqbal Z, Mahmood R. Interaction of mancozeb with human hemoglobin: spectroscopic, molecular docking and molecular dynamic simulation studies. Spectrochim Acta Part A Mol Biomol Spectrosc. 2022;280:121503.

73. Li N, Yang X, Chen F, Zeng G, Zhou L, Li X, et al. Spectroscopic and *in silico* insight into the interaction between dicofol and human serum albumin. Spectrochim Acta Part A Mol Biomol Spectrosc. 2022; 264:120277.

74. Meng D, Zhou H, Xu J, Zhang S. Studies on the interaction of salicylic acid and its monohydroxy substituted derivatives with bovine serum albumin. Chem Phys. 2021;546:111182.

75. Fliszár-Nyúl E, Faisal Z, Skaper R, Lemli B, Bayartsetseg B, Hetényi C, et al. Interaction of the emerging mycotoxins beauvericin, cyclopiazonic acid, and sterigmatocystin with human serum albumin. Biomolecules. 2022;12:1106.

76. Gu J, Zheng S, Huang X, He Q, Sun T. Exploring the mode of binding between butylated hydroxyanisole with bovine serum albumin: multispectroscopic and molecular docking study. Food Chem. 2021;357:129771.

77. Raza M, Jiang Y, Ahmad B, Rahman AU, Raza S, Khan A, et al. Biophysical investigation of interactions between sorbic acid and human serum albumin through spectroscopic and computational approaches. New J Chem. 2021;45:7682–93.

78. Lv X, Jiang Z, Zeng G, Zhao S, Li N, Chen F, et al. Comprehensive insights into the interactions of dicyclohexyl phthalate and its metabolite to human serum albumin. Food Chem Toxicol. 2021;155: 112407.

79. Kooravand M, Asadpour S, Haddadi H, Farhadian S. An insight into the interaction between malachite green oxalate with human serum albumin: molecular dynamic simulation and spectroscopic approaches. J Hazard Mater. 2021;407:124878.

80. Qi X, Xu D, Zhu J, Wang S, Peng J, Gao W, et al. Studying the interaction mechanism between bovine serum albumin and lutein dipalmitate: multi-spectroscopic and molecular docking techniques. Food Hydrocoll. 2021;113:106513.

81. Dixit S, Zia MK, Siddiqui T, Ahsan H, Khan FH. Interaction of organophosphate pesticide chlorpyrifos with alpha-2-macroglobulin: biophysical and molecular docking approach. J Immunoass Immunochem. 2021;42:138–53.

82. Golianová K, Havadej S, Verebová V, Uličný J, Holečková B, Staničová J. Interaction of conazole pesticides epoxiconazole and prothioconazole with human and bovine serum albumin studied using spectroscopic methods and molecular modeling. Int J Mol Sci. 2021;22:1925.

83. Zargar S, Wani TA. Exploring the binding mechanism and adverse toxic effects of persistent organic pollutant (dicofol) to human serum albumin: a biophysical, biochemical and computational approach. Chem Biol Interact. 2021;350:109707.

84. Su X, Wang L, Xu Y, Dong L, Lu H. Study on the binding mechanism of thiamethoxam with three model proteins:spectroscopic studies and theoretical simulations. Ecotoxicol Environ Saf. 2021;207: 111280.

85. Rahman AJ, Sharma D, Kumar D, Pathak M, Singh A, Kumar V, et al. Spectroscopic and molecular modelling study of binding mechanism of bovine serum albumin with phosmet. Spectrochim Acta Part A Mol Biomol Spectrosc. 2021;244:118803.

86. Kaur L, Rahman AJ, Singh A, Pathak M, Datta A, Singhal R, et al. Binding studies for the interaction between hazardous organophosphorus compound phosmet and lysozyme: spectroscopic and in-silico analyses. J Mol Liq. 2022;355:118954.

87. Hussain I, Fatima S, Ahmed S, Tabish M. Deciphering the biomolecular interaction of β-resorcylic acid with human lysozyme: a biophysical and bioinformatics outlook. J Mol Liq. 2022;346:117885.

88. Rostamnezhad F, Hossein Fatemi M. Exploring the interactions of acenaphthene with bovine serum albumin: spectroscopic methods, molecular modeling and chemometric approaches. Spectrochim Acta Part A Mol Biomol Spectrosc. 2021;263:120164.

89. Al-Shabib NA, Khan JM, Malik A, Rehman MT, AlAjmi MF, Husain FM, et al. Molecular interactions of food additive dye quinoline yellow (Qy) with alpha-lactalbumin: spectroscopic and computational studies. J Mol Liq. 2020;311:113215.

90. Mahmoudpour M, Javaheri-Ghezeldizaj F, Yekta R, Torbati M, Mohammadzadeh-Aghdash H, Kashanian S, et al. Thermodynamic analysis of albumin interaction with monosodium glutamate food additive: insights from multi-spectroscopic and molecular docking approaches. J Mol Struct. 2020; 1221:128785.

91. Javaheri-Ghezeldizaj F, Soleymani J, Kashanian S, Ezzati Nazhad Dolatabadi J, Dehghan P. Multi-spectroscopic, thermodynamic and molecular dockimg insights into interaction of bovine serum albumin with calcium lactate. Microchem J. 2020;154:104580.

92. Bai J, Ma X, Sun X. Investigation on the interaction of food colorant Sudan III with bovine serum albumin using spectroscopic and molecular docking methods. J Environ Sci Health A Tox Hazard Subst Environ Eng. 2020;55:669–76.

93. Rao H, Qi W, Su R, He Z, Peng X. Mechanistic and conformational studies on the interaction of human serum albumin with rhodamine B by NMR, spectroscopic and molecular modeling methods. J Mol Liq. 2020;316:113889.

94. Shamsi A, Ahmed A, Khan MS, Al Shahwan M, Husain FM, Bano B. Understanding the binding between rosmarinic acid and serum albumin: *in vitro* and *in silico* insight. J Mol Liq. 2020;311: 113348.

95. Zhou Z, Hu X, Hong X, Zheng J, Liu X, Gong D, et al. Interaction characterization of 5–hydroxymethyl–2–furaldehyde with human serum albumin: binding characteristics, conformational change and mechanism. J Mol Liq. 2020;297:111835.

96. Dahiya V, Anand BG, Kar K, Pal S. *In vitro* interaction of organophosphate metabolites with bovine serum albumin: a comparative ^{1}H NMR, fluorescence and molecular docking analysis. Pestic Biochem Physiol. 2020;163:39–50.

97. Zhao H, Bojko B, Liu F, Pawliszyn J, Peng W, Wang X. Mechanism of interactions between organophosphorus insecticides and human serum albumin: solid-phase microextraction, thermodynamics and computational approach. Chemosphere. 2020;253:126698.

98. Zhang J, Wang Z, Xing Y, Hou C, Zhou Q, Sun Y, et al. Mechanism of the interaction between benthiavalicarb-isopropyl and human serum albumin. Spectrosc Lett. 2020;53:360–71.

99. Ahmad MI, Potshangbam AM, Javed M, Ahmad M. Studies on conformational changes induced by binding of pendimethalin with human serum albumin. Chemosphere. 2020;243:125270.

100. Bai J, Sun X, Ma X. Interaction of tebuconazole with bovine serum albumin: determination of the binding mechanism and binding site by spectroscopic methods. J Environ Sci Health B. 2020;55: 509–16.

101. Chen H, Wang Q, Cai Y, Yuan R, Wang F, Zhou B. Investigation of the interaction mechanism of perfluoroalkyl carboxylic acids with human serum albumin by spectroscopic methods. Int J Environ Res Public Health. 2020;17:1319.

102. Zhang H, Deng H, Wang Y. Comprehensive investigations about the binding interaction of acesulfame with human serum albumin. Spectrochim Acta Part A Mol Biomol Spectrosc. 2020;237:118410.